THREE-PHASE AC-DC SPWM CONVERTER-FED DC SERIES MOTOR DRIVE

A Thesis Submitted
In Partial Fulfilment of the Requirements
for the Degree of

MASTER OF TECHNOLOGY

by

SUBHANKAR SANYAL

to the

DEPARTMENT OF ELECTRICAL ENGINEERING
INDIAN INSTITUTE OF TECHNOLOGY, KANPUR
MAY, 1985

DEDICATED

TO

MY UNCLE

SRI DHIRAJ KUMAR SANYAL

CERTIFICATE

This is to certify that this thesis entitled 'THREE-PHASE AC - DC SPWM CONVERTER-FED DC SERIES MOTOR DRIVE' has been carried out by Mr. Subhankar Sanyal under my supervision and this has not been submitted elsewhere for a degree.

May, 1985

(S.R. Doradla)
Assistant Professor
Electrical Engineering Department
Indian Institute of Technology
KANPUR

ABSTRACT

The performance characteristics of a three-phase ac-dc PWM converter-controlled separately excited dc motor running under reverse regenerating operation are obtained neglecting commutation transients. Since, separately excited dc motors with armature voltage control provide constant torque operation, the external performance is also determined for constant torque, under regenerating operation. The performance characteristics relating to motoring operation are also included [19]. The three-phase PWM converter motor drive system is analysed taking commutation effects also into account in regenerating operation. The analysis reveals twenty seven common modes in one repetitive period of the output voltage. The sequence of modes in one period of output voltage is established.

The external performance characteristics of a three-phase ac-dc pulse width modulated (PWM) converter controlled dc series motor are obtained for different speeds and different values of modulation index, neglecting commutation transients. Since dc series motors are commonly used for constant power operation, the performance characteristics for the series motor are also obtained with different values of constant power output. The magnetization characteristic is represented by a fifth degree polynomial.

The converter circuit is built and its performance is experimentally tested using a digital firing scheme. Speed-torque characteristics are obtained experimentally. There is a good agreement between computed and experimental results. Experimental oscillograms of typical waveforms are illustrated to verify the basic principles of operation. Although the converter circuit requires some additional components in comparison with the commonly used phase controlled converter, the improved performance characteristics make it attractive for industrial applications involving medium and large power ratings.

ACKNOWLEDGEMENTS

I am deeply indebted to Dr. S.R. Doradla for his able guidance and constant encouragement throughout the course of this project.

I wish to thank Dr. A. Mahanta for taking the photographs presented in this thesis.

I sincerely thank Mr. U.K. Mukhopadhyaya for his encouragement and help at different stages of this work.

I would like to acknowledge the ideas,suggestions and help I obtained from Mr. S.P. Yeotikar, Mr. B.H. Khan and Ms. C. Nagamani.

I am also thankful to my friends, innumerable to name, for making my stay at IIT Kanpur a pleasant chapter of my life. In this connection I would like to make a special mention of Amitabhada, Poolak, Goutam, Nandi, Satya, Saibal, Sushil, Bharti and the D-toppers/V.

Thanks are also due to Mr. C.M. Abraham for neat and quick typing of the thesis.

SUBHANKAR SANYAL

CONTENTS

List of Figures

CHAPTER I

INTRODUCTION

1.1 INTRODUCTION

Direct current (dc) motors have been used in variable-speed drives for a long time. The versatile control characteristics of dc motors have contributed to their extensive use in industry. It is well known that separately excited dc motors provide constant torque by armature voltage control upto the rated speed and constant power output by field flux control beyond the rated speed. DC series motors can generate high starting torques which are essential for traction drives. Large range of speed control can be obtained both below and above the rated speed of a dc motor. The speed control of a dc motor is simpler and less expensive than that of an ac motor. Thyristor converters which give variable dc output voltage are presently used virtually in all new variable speed dc drives. Thyristor power converters employing phase delay angle control techniques are commonly used to get variable dc output voltage from fixed ac input voltage. In phase-angle-controlled converters the ac voltage is switched on at delayed phase angles to obtain reduced dc output voltage. The main disadvantages associated with such converters are : poor supply power factor specially at large phase angle delays; generation of considerable

amount of lower order harmonic currents in the ac supply line; generation of ripple in the output current. The main advantage is the simplicity of commutation. Various methods of improvement of supply power factor have been reported in the literature [1-4]. These schemes which are based on line commutation require special supply transformers and/or control strategies. However, ac to dc converters operating on forced commutation have been developed in recent times owing to improved performance in the supply source and the load. In forced commutation, the incoming thyristor can be switched at any instant provided it is forward biased. The outgoing thyristor is commutated by a precharged capacitor. Therefore, the output voltage is not varied by delayed phase angles. The control strategy is such that the displacement angle is always held at zero as the output voltage is varied from the maximum to the minimum possible value. This makes the supply power factor high over the range of output voltage. In multi-pulse width modulated converters, the supply voltage is switched on and off several times in one half cycle to reduce the ripple in output current. The range of continuous conduction is more in such converters. Among the various modulation strategies such as equal pulse width modulation, sinusoidal pulse width modulation, inverted sine modulation, trapezoidal modulation, square-wave modulation etc. the sinusoidal pulse width modulation (SPWM) is the most desirable scheme since it improves the

ac supply current waveform and reduces the harmonic components.

DC drives of medium and large horse power are fed from three-phase ac supply system via thyristor converters. The analysis of a three-phase ac to dc SPWM converter controlled separately excited dc motor has already been done for the motoring operation [5]. Since the converter can be operated in the inversion, it is felt to make the work complete by including the reverse regeneration of a separately excited dc motor. For the sake of completeness, the external performance characteristics obtained for the motoring operation have also been shown in this thesis alongwith those obtained for reverse regeneration.

A dc series motor produces high torque at low speed and low torque at high speed. Such a characteristic makes it highly suitable for traction purposes. In the case of three-phase ac traction and also in industrial drives of medium and large power ratings where dc series motors are required as in cranes, special machine-tool drives etc. it is desirable to drive the dc series motors from three-phase converters which give variable voltage dc from three-phase ac system which is the common industrial supply. The object of the present work is to analyse a three-phase ac-dc SPWM converter-fed dc series motor. The difficulty encountered in the analysis of a dc series motor arises because of the nonlinear relationship

between the armature induced emf and the speed of the motor. The solution of the simultaneous nonlinear differential equations related to series motor operation needs numerical methods and requires much computer time. A simple but highly efficient method [6] has been adopted which saves a considerable amount of computer time without sacrificing the accuracy. In this method an analytical expression relating the speed and the current is obtained by neglecting the variation in speed and assuming the mutual inductance between the armature and the field to be a function of average current rather than instantaneous current. The converter and its control circuit are constructed. The sinusoidal pulse width modulations scheme has been implemented using digital firing scheme. The speed-torque characteristics have been verified experimentally. Oscillograms of typical waveforms from the experimental set-up are illustrated to demonstrate the satisfactory working of the experimental set-up.

1.2 OUTLINE OF THE THESIS

In Chapter II the three-phase converter circuit suitable for PWM technique and the generation of firing and extinction angles according to sinusoidal pulse width modulation have been described. A versatile digital firing scheme has been explained in detail. Experimental oscillograms depicting the current and voltage waveforms are also shown.

Chapter III deals with the analysis of a three-phase ac-dc SPWM converter controlled dc separately excited motor running under regenerative mode of operation. Supply performances such as power factor, displacement factor, harmonic factor, supply current harmonic spectrum and the load performances such as ripple factor, peak factor, range of continuous conduction etc. are determined neglecting commutation transients. Performance characteristics under constant torque operation have also been investigated. Mode analysis of the converter is also investigated taking the switching transients into account.

In Chapter IV external performance characteristics of a dc series motor fed from the same converter have been studied. A fifth degree polynomial curve is fitted into the experimental points obtained for the magnetisation characteristics of the dc series motor. Speed variation of the motor due to pulsed voltage input is neglected. The mutual inductance between the armature and field is assumed to be a function of average current and the input and output performances of the drive system are analysed. Performance characteristics under constant power operations are also determined.

Conclusions drawn and recommendation for further work are given in Chapter V.

CHAPTER II

CONVERTER CIRCUIT CONFIGURATION EMPLOYING SINUSOIDAL PULSE WIDTH MODULATION (SPWM) CONTROL TECHNIQUE

2.1 INTRODUCTION

Thyristor ac-dc converters of the phase-control type are extensively used because these converters need no special means for commutation and the operation is stable. However, such converters have inherent shortcomings that the power factor decreases as the phase control angle increases and lower harmonics of the current drawn from the ac line are relatively large. As a method for improving these shortcomings, converters of pulse width control type have been developed in recent years [7-9]. The modulation techniques employed in these converters were based on selectively improving certain input and output performances such as selective input harmonic elimination, maximum supply power factor, continuous armature current etc. In pulse width modulation (PWM) scheme, a thyristor is turned on and off several times during each half-cycle. The width of the pulse is varied to change the output voltage. In an ac-dc thyristor converter operating on forced commutation different pulse width modulation strategies such as equal pulse width modulation, sinusoidal pulse width modulation, inverted sine

modulation, trapezoidal modulation, square wave modulation etc. are possible. The sinusoidal pulse width modulation (SPWM) is by far the most desirable scheme since it improves the ac supply current waveform and reduces harmonic components. The converter circuits reported so far have been studied mostly on single-phase ac supply system. However, a versatile converter circuit operating on complementary voltage commutation was reported by Kataoka et al. [10]. This circuit has the following advantages over the other PWM-controlled converter circuits reported in the literature:

it does not have complex commutation circuits using auxiliary thyristors ; the adjustable range of output voltage is larger even when the converter operates under light load; regenerative operation is also possible.

2.2 CONVERTER CIRCUIT CONFIGURATION

Fig. 2.2.1 shows the three-phase converter circuit [10] suitable for implementing SPWM control technique. Thyristors T_1 to T_3 are commutated by complementary voltage impulse commutation while thyristors T_5 to T_6 are line commutated. Diodes D_{L1} to D_{L3}, inductors L_1 to L_3 and capacitors C_1 to C_3 are the commutating elements used to implement the PWM scheme. The diodes D_1 to D_3 prevent the commutating capacitors from discharging into the load completely. L_s is the source inductance in each phase, to ensure commutation even at low

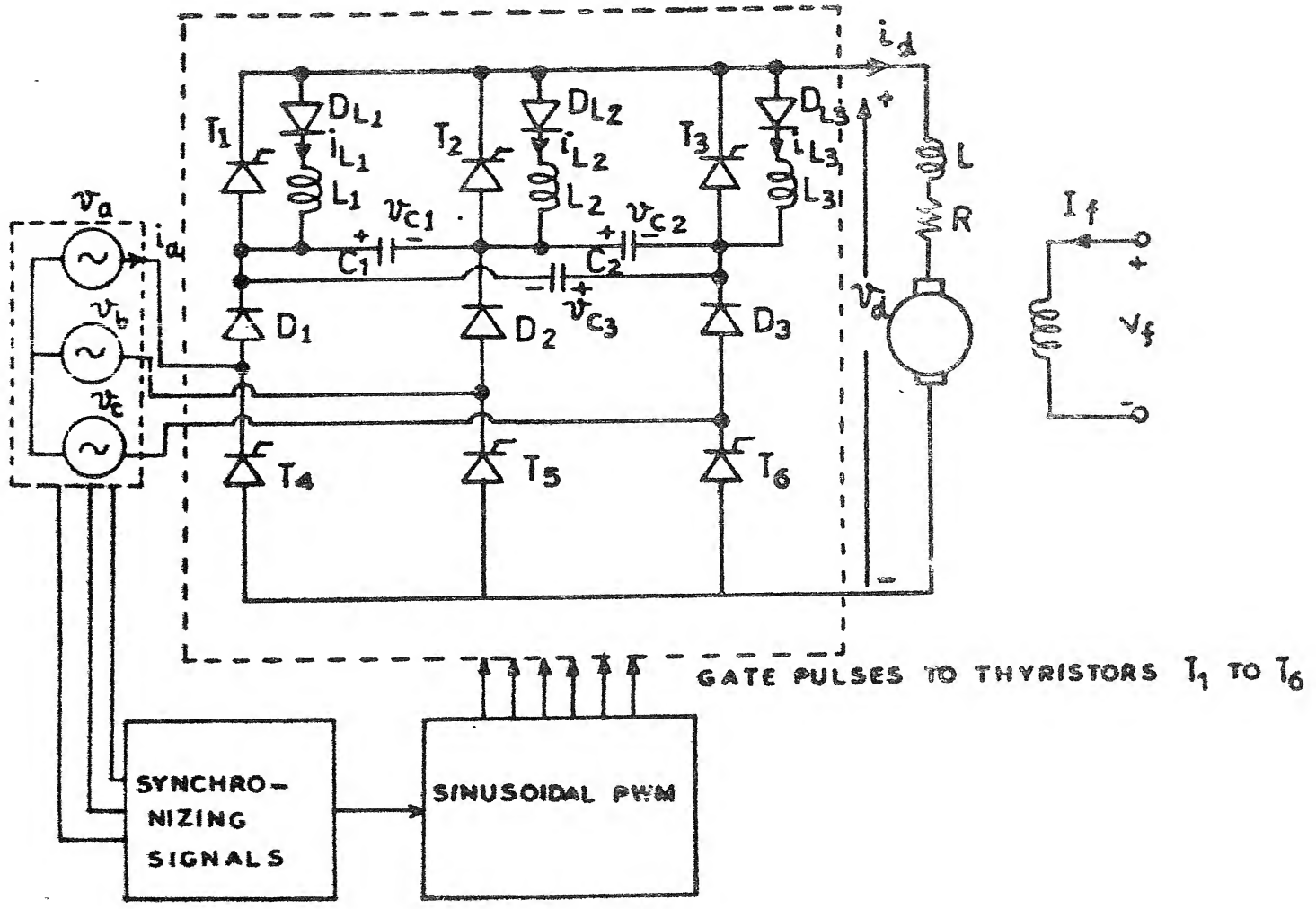

FIG. 2.21 THREE PHASE AC-DC CONVERTER EMPLOYING SINUSOIDAL PULSE WIDTH MODULATION (SPWM)

supply voltages. T_1 to T_3 are turned on and off several times in each cycle of the supply voltage. Therefore, they must be of inverter grade. The line commutated thyristors T_4 to T_6 can be of converter grade.

The modulation scheme employs four pulses per half cycle of each phase of the supply voltage. The gating pulses to thyristors T_1 to T_6 are obtained by comparing a carrier signal (triangular) with a modulating signal (three phase rectified wave). With six pulses per half cycle of the supply voltage, the frequency of the carrier wave is twelve times the frequency of the supply voltage. Fig. 2.2.2(a) shows the generation of the gate pulses for motoring mode while Fig. 2.2.2(b) shows the same for regenerating mode. Whenever two thyristors in the same leg of the converter circuit conducts free-wheeling of the load current takes place. The armature current decays in motoring operation while it rises up in the regenerating operation. On the other hand, if two thyristors in different legs, one in the top group and other in the bottom group, conduct, power is supplied to the load circuit in the motoring mode while it is returned to the line in regenerating mode.

2.3 FIRING AND EXTINCTION ANGLES

Firing (α's) and extinction (β's) angles are determined by comparing the carrier wave with the modulating wave. The modulation index (M) is defined as the ratio of the peak

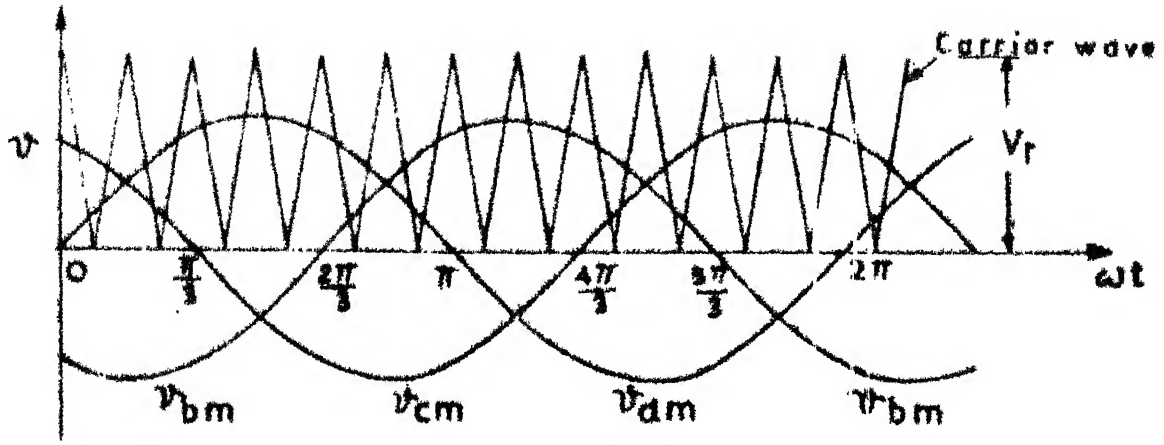

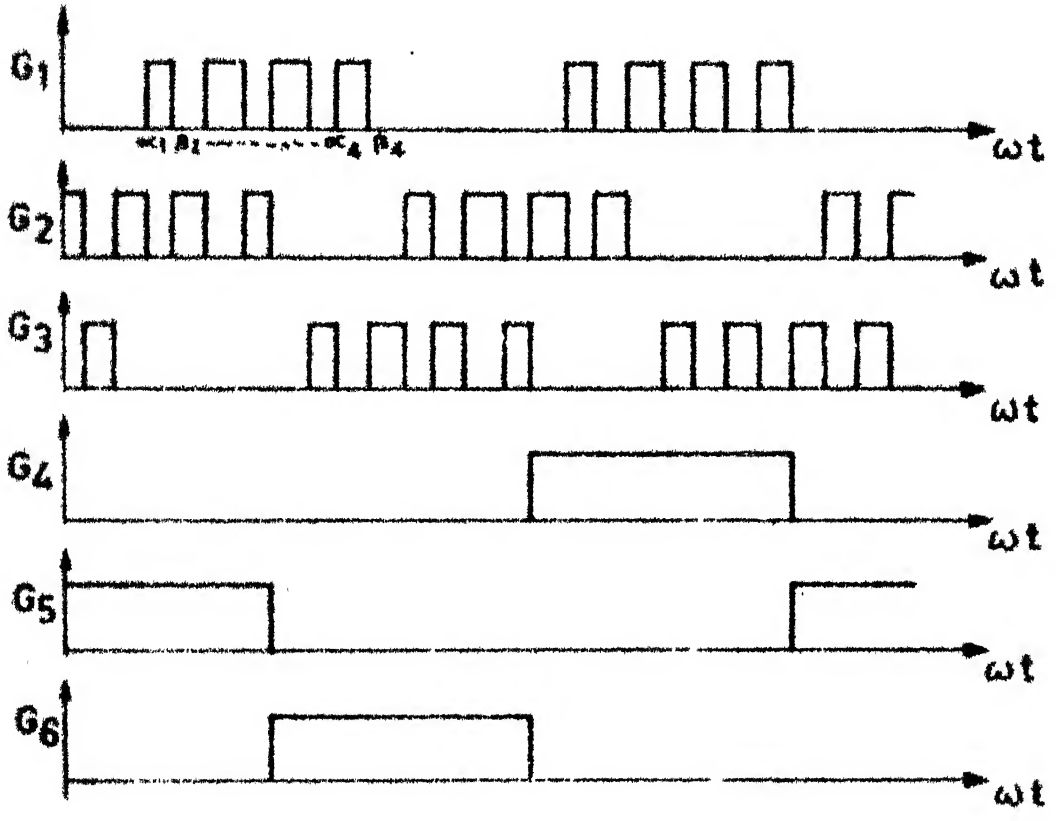

FIG. 2.2.2 (a) MOTORING OPERATION

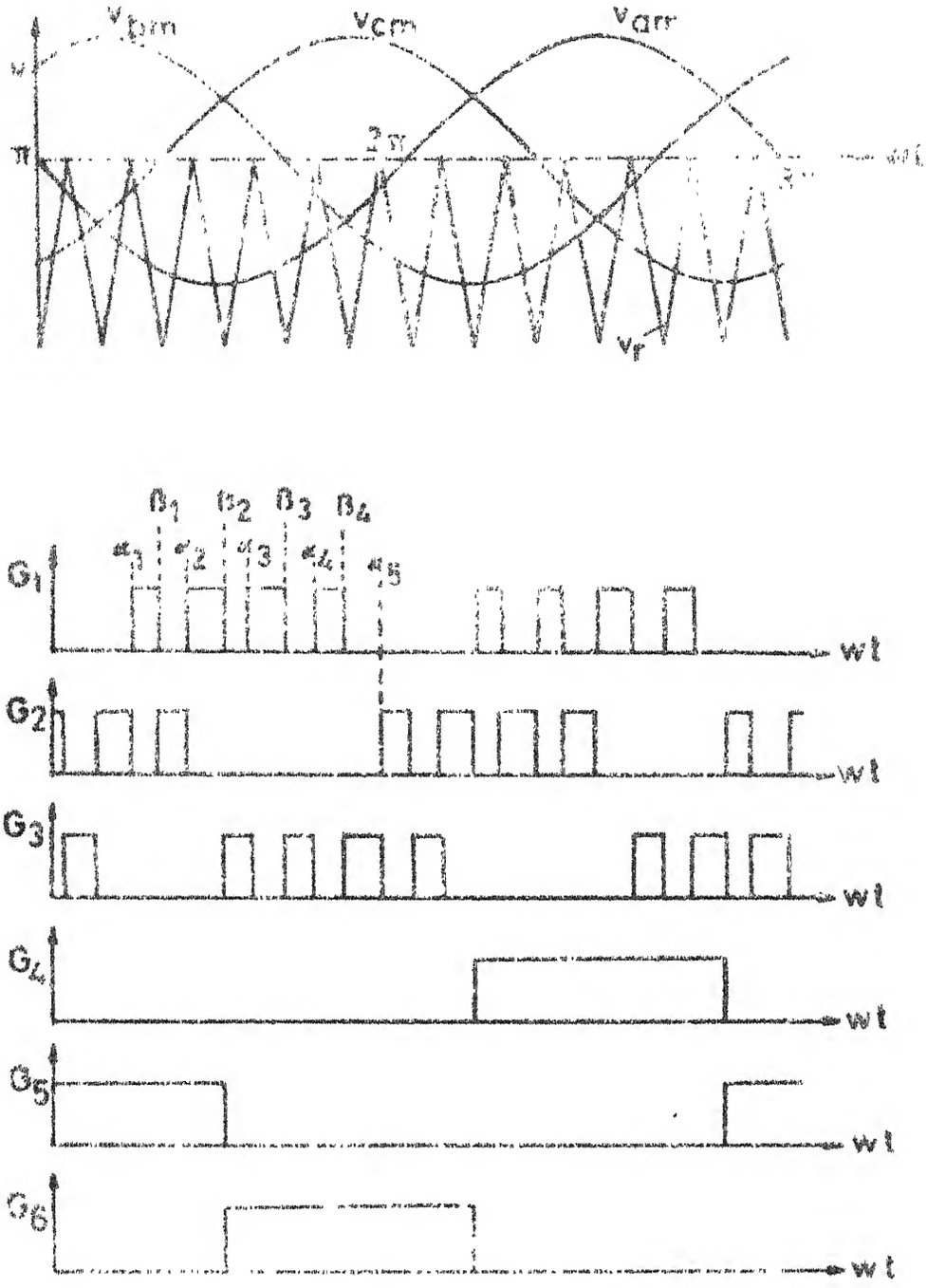

FIG 3.2.2(b) GENERATION OF GATE PULSES FOR THYRISTORS $T_1 - T_6$ FOR REGENERATING OPERATION

amplitude of the modulating wave (V_m) to the peak amplitude of the carrier wave (V_r). That is,

$$M = V_m/V_r \tag{2.3.1}$$

The modulating wave (v_{am}) and Kth carrier wave (v_{ark}) for the phase a, are

$$v_{am}(\theta) = M \sin(\gamma+\pi/6), \quad \gamma = \theta \text{ for motoring}$$
$$\gamma = (\pi+\theta) \text{ for regeneration}$$
$$\theta = \omega t \tag{2.3.2}$$

$$v_{ark}(\theta) = \pm ((2p/\pi)\theta - (2K-1)\theta) \tag{2.3.3}$$

p = number of pulses per half cycle of supply voltage = 6

The positive and negative slopes in equation (2.3.3) are used to determine α's and β's. Equating eqn. (2.3.2) and eqn. (2.3.3) two nonlinear equations (2.3.4) and (2.3.5) are obtained.

$$M \sin(\alpha'_{ak}+(\pi/6))+(2P/\pi)\ \alpha'_{ak}-(2K-1) = 0 \tag{2.3.4}$$

$$M \sin(\beta'_{ak}+(\pi/6))-(2P/\pi)\beta'_{ak}+(2K-1) = 0 \tag{2.3.5}$$

where, $\alpha_{ak} = \alpha'_{ak} + (\pi/6)$ for motoring operation

$= \alpha'_{ak} + (7\pi/6)$ for regenerating operation

$$\beta_{ak} = \beta'_{ak} + (\pi/6) \quad \text{for motoring operation}$$

$$= \beta'_{ak} + (7\pi/6) \quad \text{for regenerating operation}$$

The nonlinear equations (2.3.4) and (2.3.5) are solved by Newton-Raphson method for firing and extinction angles corresponding to pulses K = 1,2, ..., 2P/3 for the phase a.

An expression for the average output voltage, V_{dc} can be easily derived knowing firing and extinction angles.

$$V_{dc} = \frac{3}{\pi} \int_{\pi/6}^{\pi/2} v_{ab}(\theta)\, d\theta$$

$$= \frac{3\sqrt{6}\,V}{\pi} \int_{\pi/6}^{\pi/2} \sin(\theta+\pi/6)\, d\theta$$

$$= \frac{3\sqrt{6}\,V}{\pi} \sum_{Ka=1}^{P/3} (\cos(\alpha_{Ka}+\pi/6)-\cos(\beta_{Ka}+\pi/6)) \quad (2.3.6)$$

From eqn. (2.3.6) it can be seen that the dc output voltage is a function of the firing and extinction angles which in turn depend upon the number of pulses and the modulation index. Fig. 2.3.1 shows the variation of the dc component of output voltage with modulation index is linear. This is advantageous specially when the converter is operated in a closed loop control.

Fig. 2.3.2 shows typical output voltage waveform for motoring and regenerating operations. Typical input and output voltage waveforms obtained from the experimental set up are

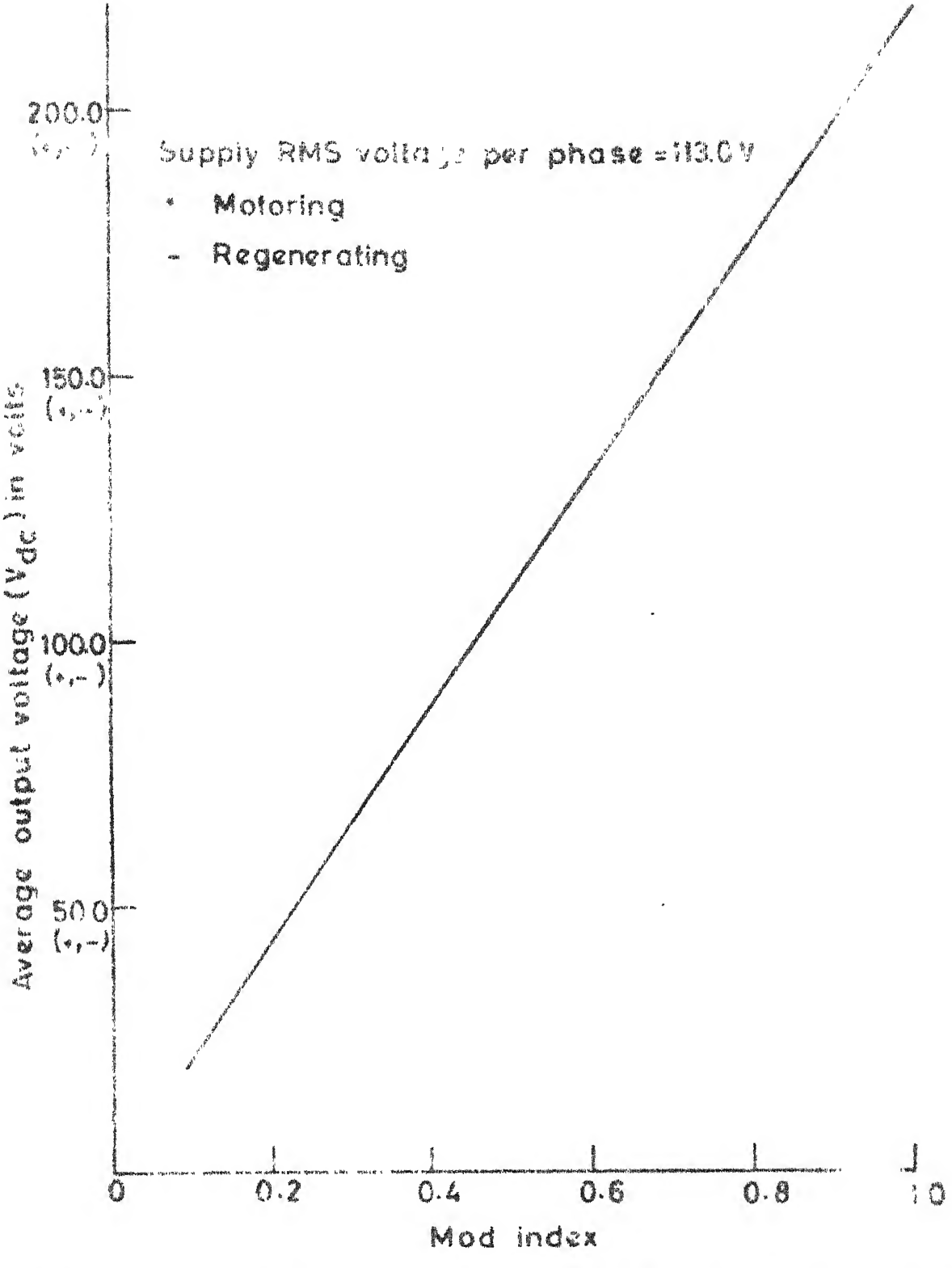

FIG. 2.3.1 AVERAGE OUTPUT VOLTAGE VS MODULATION INDEX

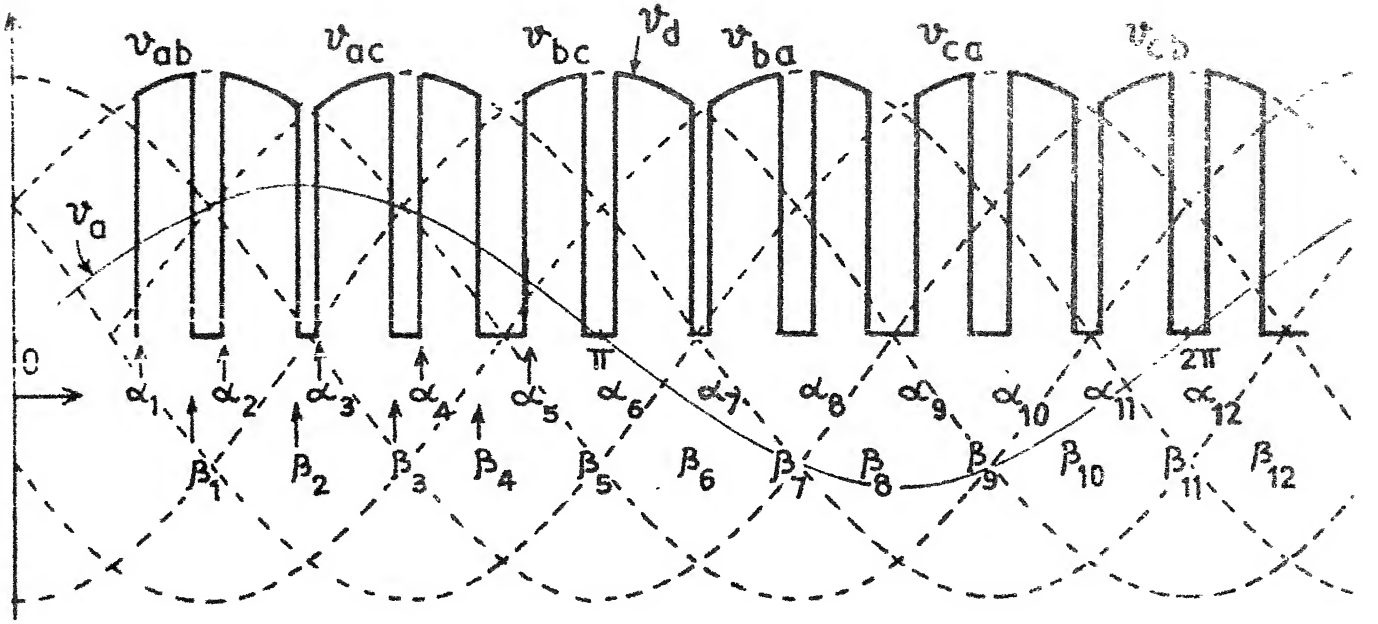

Repetitive period in the output Voltage : α_1 to α_5

Firing angles : α's

Extinction angles : β's.

FIG. 2.3.2 (a) MOTORING OPERATION

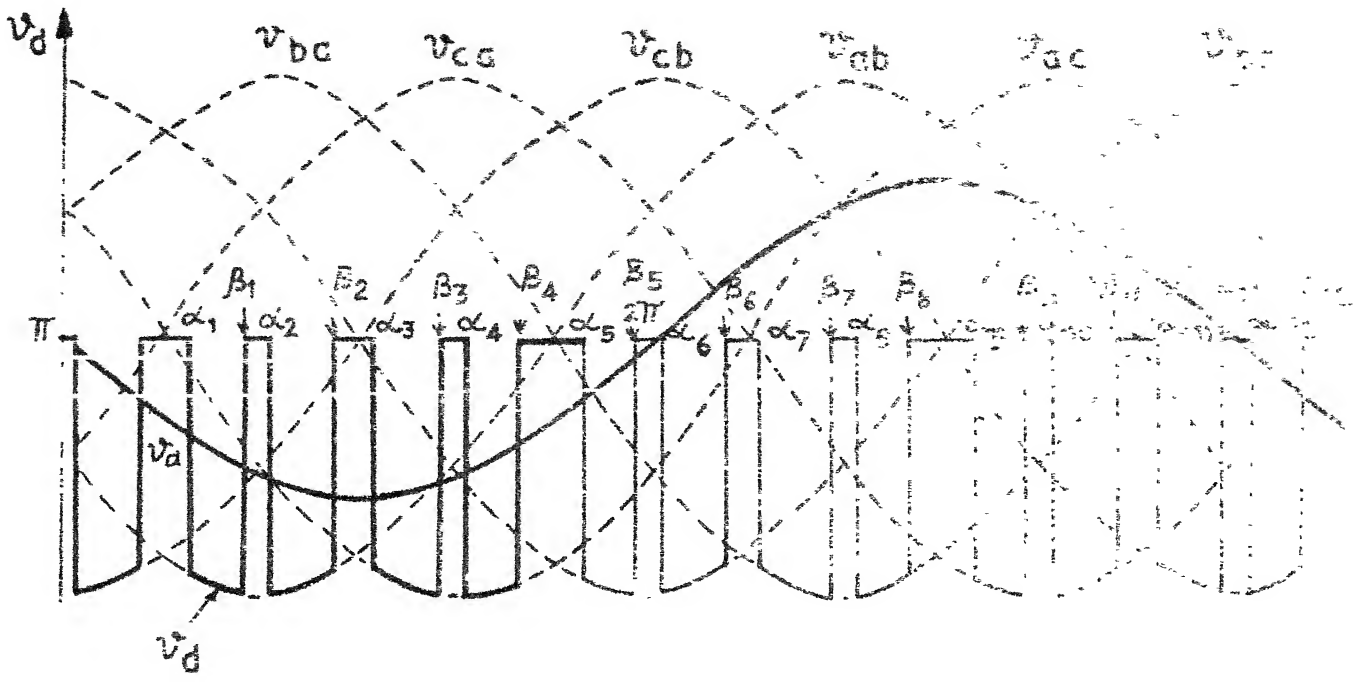

REPETITIVE PERIOD IN OUTPUT VOLTAGE : α_1 to α_8

FIRING ANGLES : α's

EXTINCTION ANGLES : β's

FIG 2.3.2 (b) OUTPUT VOLTAGE WAVEFORM OF A THREE PHASE FULL SPWM AC-DC CONVERTER, REGENERATIVE MODE OF OPERATION

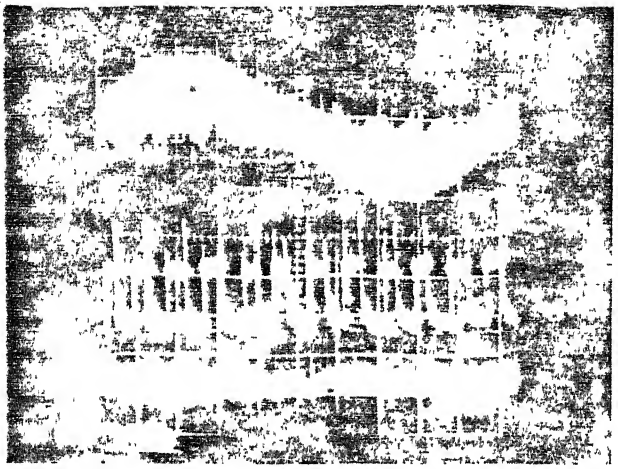

– ϑ_a : 200 V/div
i_a : 6.1 A/div

– ϑ_d : 100 V/div

– i_d = 3.7 A/div

(a) Motoring M = 0.7 , N = 900 RPM

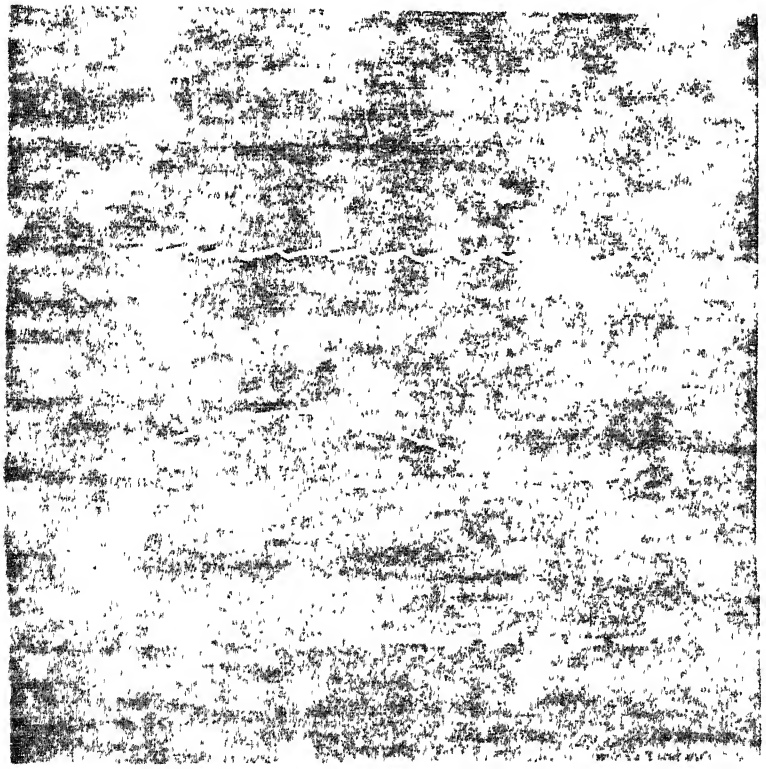

– ϑ_d : 20ϑ/div

– i_d : 3 A/div

– ϑ_a : 20 ϑ/div

– i_a = 1.22 A/div

(b) Regenerating M = 0.5 , N = 310 RPM

Fig 2.3.3 Typical input and output waveforms (2 mse./di

illustrated in Fig. 2.3.3(a) and (b) for motoring and regenerating operations respectively.

2.4 DIGITAL FIRING SCHEME

In the literature, some analog firing schemes are propose for the PWM-controlled converters [11], [12]. These analog firing schemes have the following drawbacks.

(i) Large number of components are required.

(ii) They are very sensitive to voltage surges, noise and line distortion

(iii) Implementation of more than one modulation strategy makes the analog firing scheme complicated and at times prohibitive.

Digital firing schemes, on the other hand, can achieve more precise and symmetrical firing with less difficulty, necessitate fewer high precision components, are more compact and reliable, consume less power and are not vulnerable to amplifier drift and offset problems. Multi-mode control strategy for optimum performance of the converter drive system is also possible in digital firing scheme with hardly any modifications in the circuit.

Design and successful implementation of the digital firing scheme (DFS) for single phase PWM converter has been reported in the literature [13]. The extension of the single-

phase DFS for three phase PWM converter has been implemented in the present work.

2.4.1 Basic Principle of Versatile Digital Firing Scheme

The block diagram of the three-phase DFS is shown in Fig. 2.4.1. It consists broadly of (a) Erasable Programmable Read Only Memory (EPROM), (b) Firing Angle Generation Counter (FAGC) and (c) Pulse Number Generation Counter (PNGC) besides other blocks such as Analog to Digital Converter (ADC), Logic circuit, isolation and pulse amplifier circuit. For a given modulation strategy, the firing and extinction angles are computed theoretically over the entire output voltage range and stored in the EPROM as a look-up table. This helps to eliminate any nonlinearity present between the control voltage and output voltage. The control voltage and the outputs of the PNGC set the address to the EPROM. The external clock frequency depends upon the supply frequency and the number of pulses per half cycle.

2.4.2 Detailed Description of Three Phase DFS

The detailed circuit diagram of the three-phase DFS is shown in Fig. 2.4.2. Pertinent waveforms and the logic circuit for motoring operation are shown in Fig. 2.4.3 and Fig. 2.4.4 respectively.

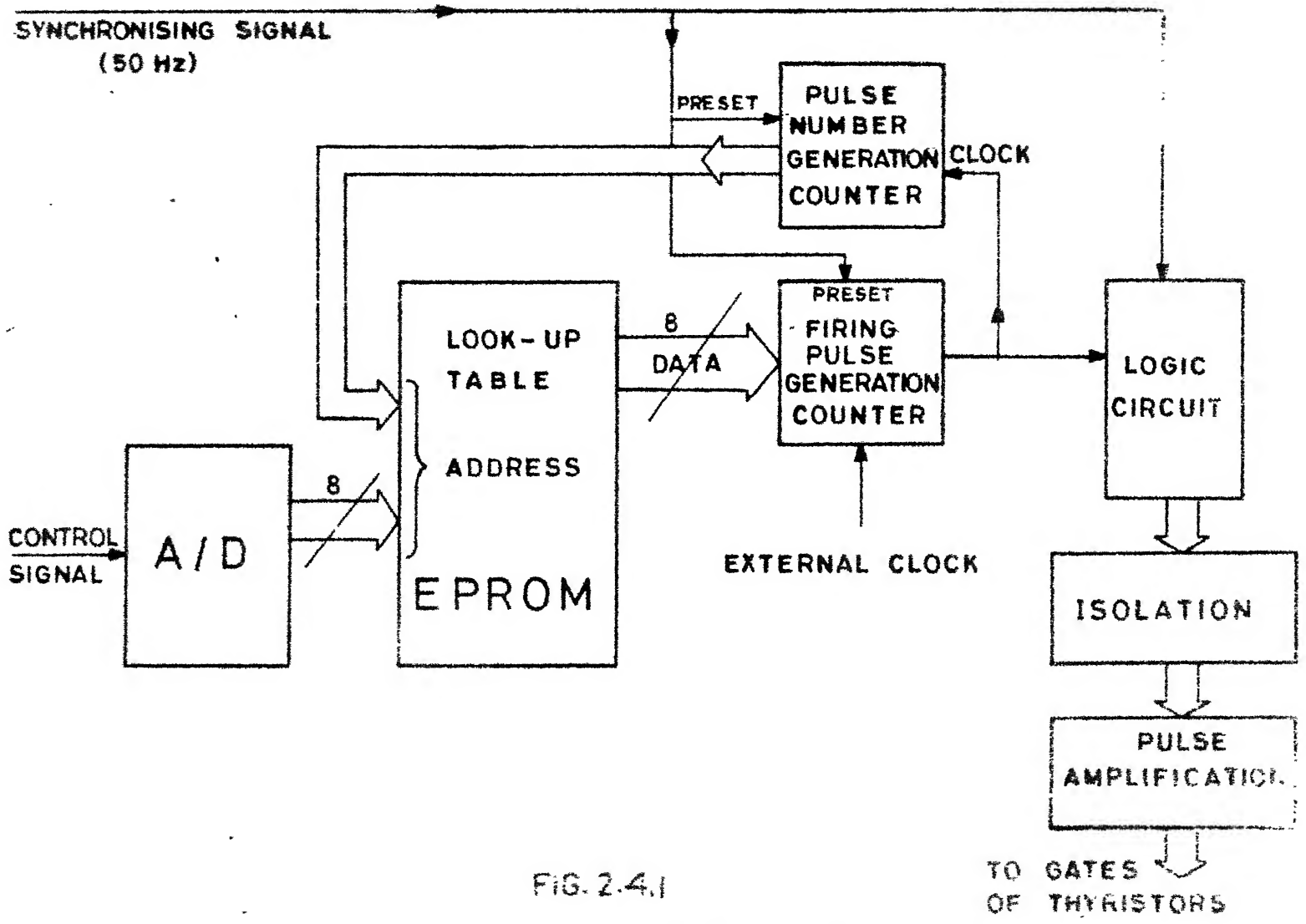

FIG. 2.4.1

BLOCK DIAGRAM OF A DIGITAL FIRING SCHEME.

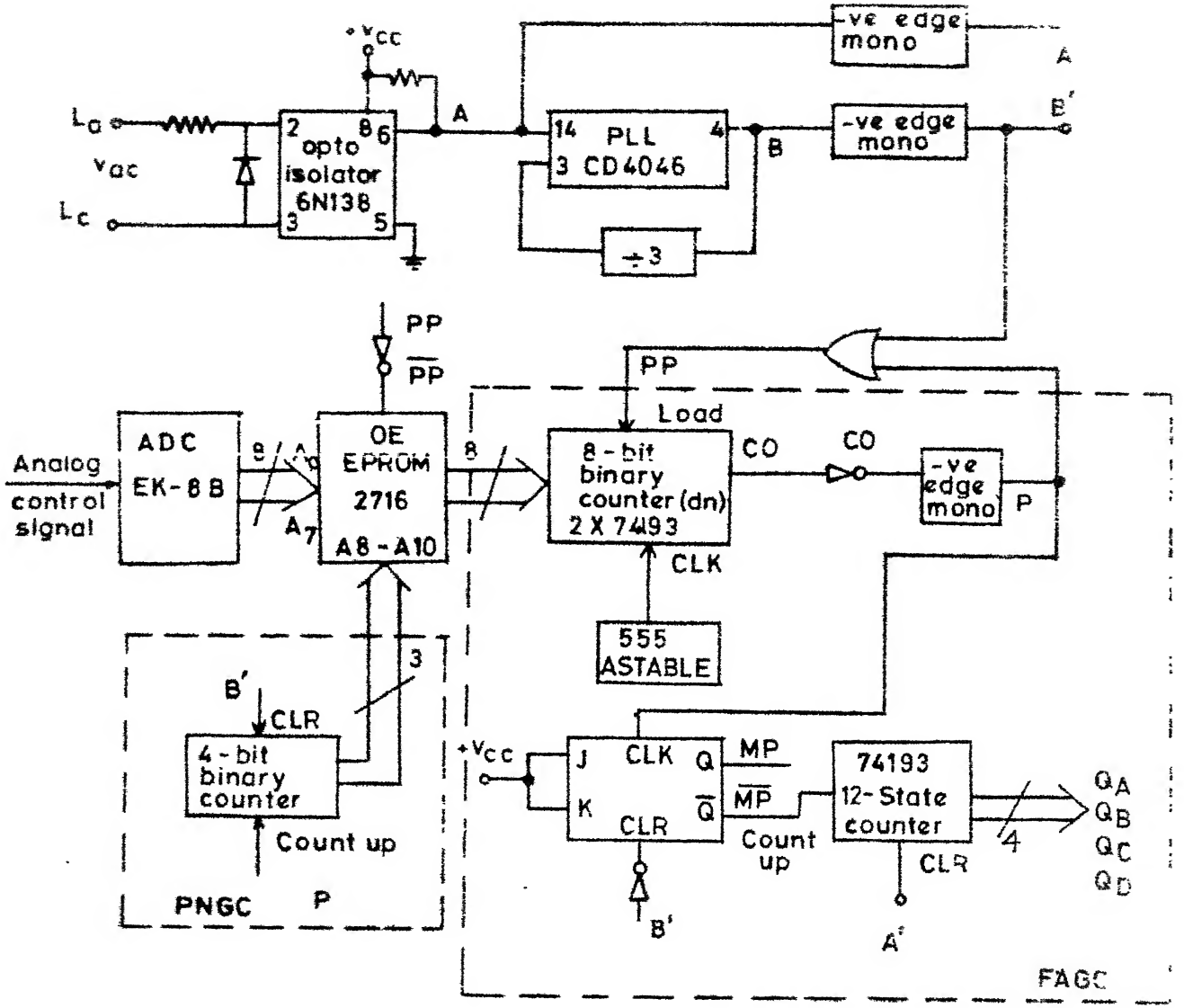

FIG. 2 - 3 CIRCUIT DIAGRAM OF THREE PHASE DIGITAL FIRING SCHEME

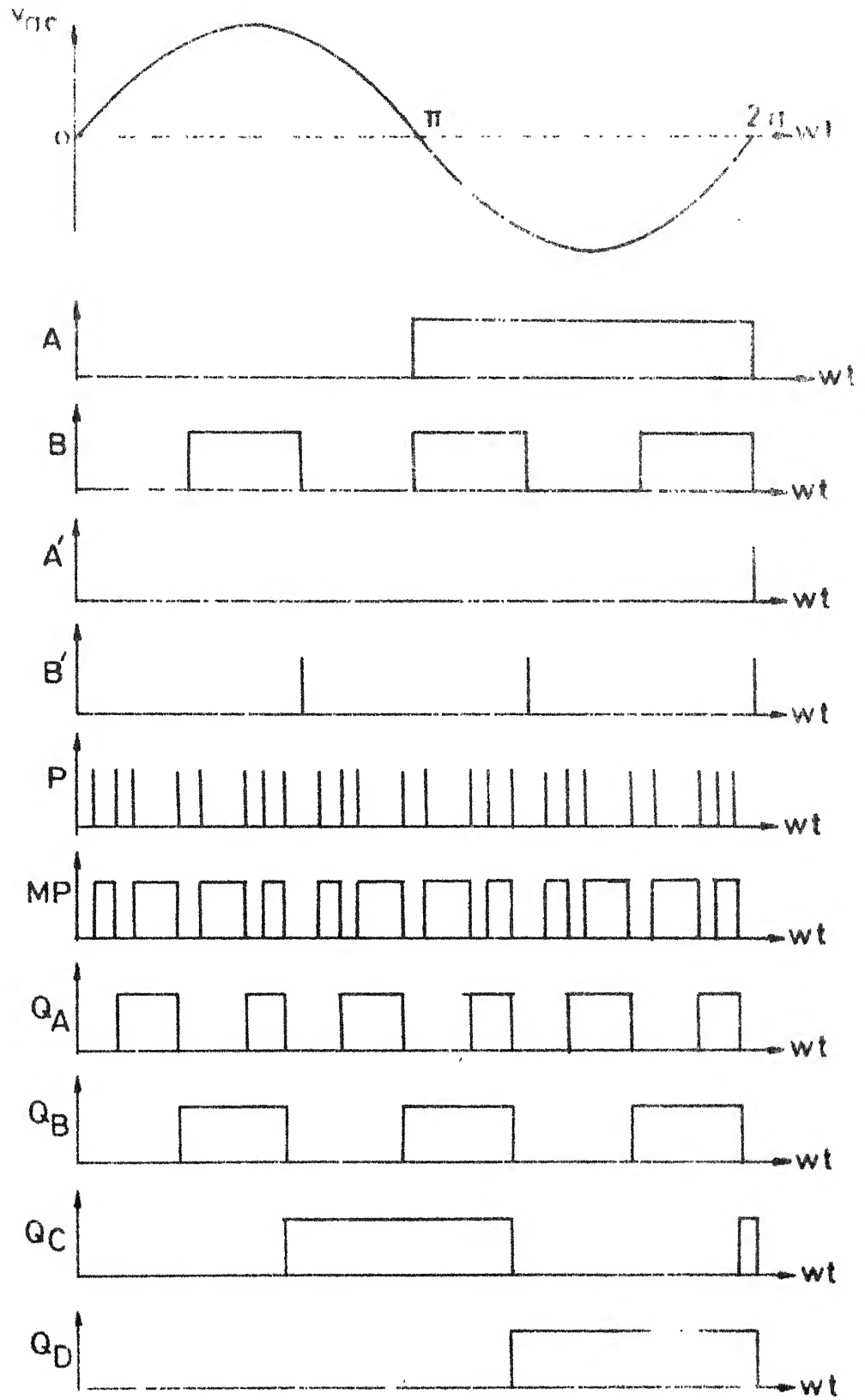

FIG. 2.4.3 SIGNALS AT VARIOUS STAGES OF FIG. 2.4.2

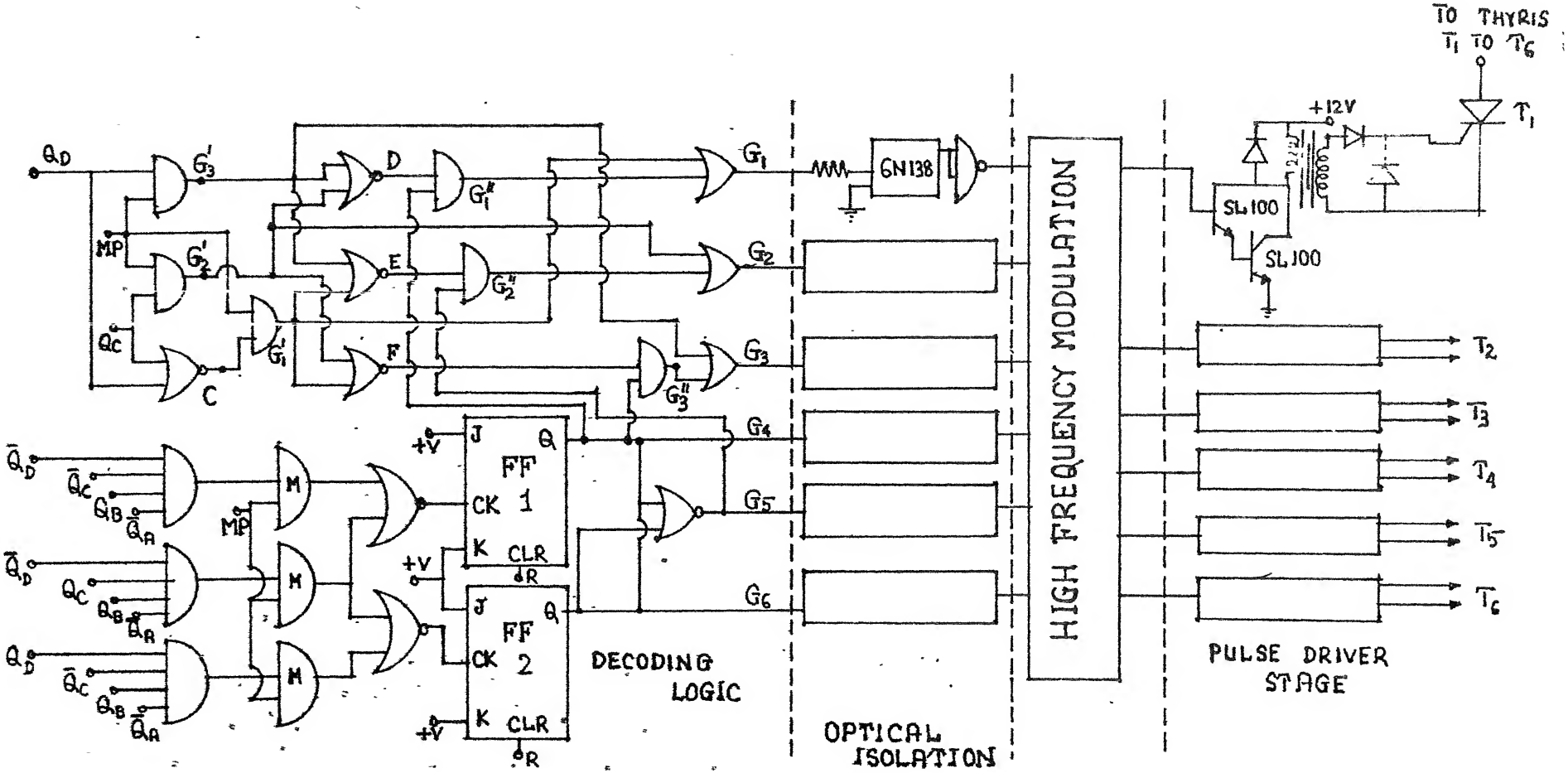

FIG.2.4.4. LOGIC CKT. DIAGRAM FOR GENERATION OF GATE PULSES.

The firing and extinction angles as computed theoretically for different modulation indices are stored as a look-up table in EPROM (2716). The supply line voltage v_{ac} is digitised using an opto-isolator to get the waveform A. Frequency of A is multiplied three times with the help of a PLL (CD4046) and a 3 counter. The output signal B of the PLL is fed to the input of a -ve edge triggered monostable to get voltage shots which are synchronised with the supply line voltage v_{ac} and are spaced 120^{o} apart from each other. The PNGC which is a simple up-mode counter (74193) is cleared after every 120^{o} interval. The lower eight address bits (A_7 ... A_0) of the EPROM correspond to the modulation index and are determined by the analog control signal via the ADC (EK-8B). The PNGC sets the upper three address bits (A_{10} ... A_8). The amount of delay which is equivalent to the power or freewheeling interval is loaded into the 8-bit counter (2x74193) from EPROM. Counter counts down to zero and gives a carry out pulse CO is fed to a -ve edge mono to get P. These pulses P and pulses of B' which is synchronised with the line voltage are used to reload the FAGC with the next count value. CO is also used as a clock to a J-K flip flop (7473) connected in toggle mode and also as a clock to the PNGC. This J-K flip-flop is cleared at every 120^{o} interval by B'. The output of the J-K flip flop, MP is a pulsed waveform, the widths of which are equal to the desired power intervals.

From Figs. 2.2.2(a) and (b) it can be seen that gate pulses to the upper group thyristors, T_1 to T_3 are repetitive short pulses while the pulses to the bottom group thyristors, T_4 to T_6 are of long duration. Generation of gate pulses for all the six thyristors, T_1 to T_6 from the pulse-train MP with the help of a logic circuit (Fig. 2.4.4) for both motoring and regenerating operations are explained in the next two paragraphs.

The pulses, MP are coded from 0000 to 1011 by clocking a 4-bit counter (74193) with MP and clearing it with the mono-stable output E. Of these, the pulses 0010, 0110 and 1010 of the pulse train are decoded using three 4-input AND gates. A J-K flip-flop is used in toggle mode to generate a long pulse which goes high at the positive going edge of the pulse 0010 and goes low at the positive going edge of the pulse 0110. This long pulse G_6 is the gate pulse for T_6. Similarly, another J-K flip-flop is used to generate G_4 which goes high at the positive going edge of the pulse 0110 and goes low at the positive going edge of the pulse 1010. The pulses G_4 and G_6 are NOR-ed to obtain G_5.

There are a total of eight pulses per cycle for each of the thyristors T_1 to T_3. And in each supply cycle there are twelve pulses in the pulse-train, MP. The first, middle and the last four pulses (G_1', G_2' and G_3') of MP are given to the

gates of the thyristors T_1,T_2 and T_3 respectively. G_1', G_2' and G_3' trigger the corresponding thyristors in the power intervals. By ANDing the signal MP with output Q_c of the 4-bit coding counter G_2' is obtained. G_3' is obtained by ANDing MP with Q_D of the same counter. Q_C and Q_D are NORed to get a signal C. C is ANDed with MP to get G_1'. G_2' and G_3' are NORed to get a signal D. D is ANDed with G_4 to give the pulse train G_1''. G_3' and G_1' are NORed to get the signal E which is ANDed with G_5 to generate G_2''. G_1' and G_2' are NORed to get the signal F. F is ANDed with G_6 to obtain G_3''. G_1'', G_2'' and G_3'' are the triggering pulses to T_1, T_2 and T_3 respectively to provide freewheeling action through these thyristors. Three 2-input OR gates with inputs G_1' and G_1'', G_2' and G_2'' and G_3' and G_3'' generate G_1, G_2 and G_3 which are the firing pulses to thyristors T_1,T_2 and T_3 respectively.

In the case of regeneration v_{ca} instead of v_{ac} is fed as an input to the optoisolator. Generation of pulse train MP is done in the same way as in the case of motoring. Coding and decoding of pulse-train MP is done in the same way. A J-K flip-flop is used in toggle mode to generate a long pulse which goes high at the falling edge of pulse 0001 and goes low at the -ve going edge of pulse 0101. This long pulse G_6 is the gate pulse to T_6. Similarly another J-K flip-flop is used to generate G_4 which goes high at the falling edge of pulse no.0101

and goes low at the falling edge of pulse no. 0101. To achieve this the three AND gates marked 'M' in Fig. 2.4.4 are bypassed and decoded signals are directly connected to the inputs of the two NOR-gates. Pulses G_4 and G_6 are NOR-ed to get G_5. Generation of G_1 to G_3 is done in the same way as in motoring case.

The gate signals thus obtained are optically isolated and modulated with high-frequency before being fed to the driver stage. From driver stage pulses are given to the gates of respective thyristors through pulse-transformers.

CHAPTER III

EXTERNAL PERFORMANCE CHARACTERISTICS AND DETAILED ANALYSIS OF THE CONVERTER WITH A DC SEPARATELY EXCITED MOTOR LOAD RUNNING IN REGENERATIVE MODE

3.1 INTRODUCTION

In this chapter the input and output performance characteristics of a three phase ac-dc converter controlled dc separately excited motor employing forced commutation are thoroughly investigated with the motor running under regenerative mode of operation. The supply performances such as power factor, displacement factor, harmonic factor, supply current harmonic spectrum and the load performances such as ripple factor, peak current factor, range of continuous conduction are determined for different speeds and modulation indices neglecting commutation effects. Performance characteristics under motoring mode [5] have also been shown along with those for regenerative operation to facilitate a comparative study. A separately excited dc motor with armature voltage control provides constant torque characteristics. Therefore, the performance is also evaluated for different constant load torques. The speed-torque characteristics are illustrated showing the boundary between continuous and discontinuous conduction regions. The converter circuit is analysed taking

the commutation effects also into account. Because of the presence of switching devices, the converter circuit undergoes several topological modes. The converter circuit is analysed using state variable technique. Nearly twenty-seven prominent modes have been identified in each fundamental period of the output voltage under continuous output current. The mode sequence for each pulse is also given. The modes and the sequence of modes are not, however, unique. They depend upon commutation circuit parameters, source impedance and modulation index.

3.2 EXTERNAL PERFORMANCE CHARACTERISTICS

The commutation transients have been neglected while determining the steady-state current waveform and the converter circuit is assumed to operate according to the sinusoidal pulse width modulation scheme. Since, the output voltage repeats after every four pulses as is evident from Fig.2.3.2, it is sufficient to consider the current waveform for any four pulses if the steady-state performance is derived. Since, the mechanical time constant is large compared to the electrical time constant of the motor armature circuit, the speed fluctuations under steady-state can be neglected. For a given modulation index, M, the firing and extinction angles are computed as explained in Chapter II.

The instantaneous output current is calculated over a period of 120° starting from α_1 as shown in Fig. 2.3.2. This 120° span of time consists of four power intervals and four freewheeling intervals. Voltages applied across the load during the power intervals are v_{ab} for the intervals α_1 to β_1 and α_2 to β_2 and v_{ac} for the periods α_3 to β_3 and α_4 to β_4. Let the steady-state instantaneous currents at $\alpha_1,\beta_1,\alpha_2,\beta_2,\alpha_3,\beta_3,\alpha_4,\beta_4$ and α_5 be denoted as $I_1,I_2,I_3, \ldots, I_9$ respectively.

During the first power interval wherein $\alpha_1 \leq \omega t < \beta_1$ the voltage equation is

$$L\frac{di}{dt} + Ri = v_{ab}+E = \sqrt{6}V\sin(\omega t + \pi/6) \qquad (3.2.1)$$

where, L = total inductance in armature circuit

R = total resistance in armature circuit

E = motor back emf

ω = angular frequency of the ac supply

V = rms supply voltage per phase

The solution of eqn. (3.2.1) with the initial condition $i(\alpha_1) = I_1$ is

$$i = \frac{\sqrt{6}\,V}{Z}\sin(\omega t+\pi/6-\phi) + \frac{E}{R} + \left(I_1 - \frac{\sqrt{6}V}{Z}\sin(\alpha_1+\pi/6-\phi) - \frac{E}{R}\right)e^{-\frac{\omega t-\alpha_1}{Q_L}} \qquad (3.2.2)$$

where Z = impedance of armature circuit

$= (R^2+\omega^2L^2)^{1/2}$

Q_L = quality factor

$= \frac{\omega L}{R}$

ϕ = phase angle of the circuit

$= \tan^{-1} Q_L$

Using eqn. (3.2.2) I_2, the value of i at β_1 can be found.

$$i(\beta_1) = I_2 = \frac{\sqrt{6}V}{Z} \sin(\beta_1+\pi/6-\phi) + \frac{E}{R} + (I_1 - \frac{\sqrt{6}V}{Z} \sin(\alpha_1+\pi/6-\phi) - \frac{E}{R}) e^{-\frac{\beta_1-\alpha_1}{Q_L}} \quad (3.2.3)$$

During the first freewheeling interval wherein $\beta_1 \leq \omega t \leq \alpha_2$ the voltage equation is

$$L \frac{di}{dt} + Ri + E = 0 \quad (3.2.4)$$

Solution of this equation with the initial value of current $i(\beta_1) = I_2$ is

$$i = \frac{E}{R} + (I_2 - \frac{E}{R}) e^{-\frac{\omega t-\beta_1}{Q_L}} \quad (3.2.5)$$

$$I_3 = i(\alpha_2) = \frac{E}{R} + (I_2 - \frac{E}{R}) e^{-\frac{\alpha_2-\beta_1}{Q_L}} \quad (3.2.6)$$

Similarly, the equation of current for different intervals are found as follows :

$\alpha_2 \leq \omega t \leq \beta_2$

$$i = \frac{\sqrt{6}V}{Z} \sin(\omega t+\pi/6-\phi) + \frac{E}{R} + (I_3 - \frac{\sqrt{6}V}{Z} \sin(\alpha_2+\pi/6-\phi) - \frac{E}{R}) e^{-\frac{\omega t-\alpha_2}{Q_L}} \quad (3.2.7)$$

$$I_4 = i(\beta_2) = \frac{\sqrt{6}V}{Z} \sin(\beta_2+\pi/6-\phi) + \frac{E}{R} + I_3 - \frac{\sqrt{6}V}{Z} \sin(\alpha_2+\pi/6-\phi) - \frac{E}{R}) e^{-\frac{\beta_2-\alpha_2}{Q_L}} \quad (3.2.8)$$

$\beta_2 \leq \omega t \leq \alpha_3$

$$i = \frac{E}{R} + (I_4 - \frac{E}{R}) e^{-\frac{\omega t-\beta_2}{Q_L}} \quad (3.2.9)$$

$$I_5 = i(\alpha_3) = \frac{E}{R} + (I_4 - \frac{E}{R}) e^{-\frac{\alpha_3-\beta_2}{Q_L}} \quad (3.2.10)$$

$\alpha_3 \leq \omega t \leq \beta_3$

$$i = \frac{\sqrt{6}V}{Z} \sin(\omega t-\pi/6-\phi) + \frac{E}{R} + (I_5 - \frac{\sqrt{6}V}{Z} \sin(\alpha_3-\pi/6-\phi) - \frac{E}{R}) e^{-\frac{\omega t-\alpha_3}{Q_L}} \quad (3.2.11)$$

$$I_6 = i(\beta_3) = \frac{\sqrt{6}V}{Z} \sin(\beta_3-\pi/6-\phi) + \frac{E}{R} + (I_5 - \frac{\sqrt{6}V}{Z} \sin(\alpha_3-\pi/6-\phi) - \frac{E}{R}) e^{-\frac{\beta_3-\alpha_3}{Q_L}} \quad (3.2.12)$$

$\beta_3 \leq \omega t \leq \alpha_4$

$$i = \frac{E}{R} + (I_6 - \frac{E}{R})\, e^{-\frac{\omega t - \beta_3}{Q_L}} \tag{3.2.13}$$

$$I_7 = i(\alpha_4) = \frac{E}{R} + (I_6 - \frac{E}{R})\, e^{-\frac{\alpha_4 - \beta_3}{Q_L}} \tag{3.2.14}$$

$\alpha_4 \leq \omega t \leq \beta_4$

$$i = \frac{\sqrt{6}V}{Z} \sin(\omega t - \pi/6 - \phi) + \frac{E}{R} + (I_7 - \frac{\sqrt{6}V}{Z} \sin(\alpha_4 - \pi/6 - \phi) - \frac{E}{R})\, e^{-\frac{\omega t - \alpha_4}{Q_L}} \tag{3.2.15}$$

$$I_8 = i(\beta_4) = \frac{\sqrt{6}V}{Z} \sin(\beta_4 - \pi/6 - \phi) + \frac{E}{R} + (I_7 - \frac{\sqrt{6}V}{Z} \sin(\alpha_4 - \pi/6 - \phi) - \frac{E}{R})\, e^{-\frac{\beta_4 - \alpha_4}{Q_L}} \tag{3.2.16}$$

$\beta_4 \leq \omega t \leq \alpha_5$

$$i = \frac{E}{R} + (I_8 - \frac{E}{R})\, e^{-\frac{\omega t - \beta_4}{Q_L}} \tag{3.2.17}$$

$$I_9 = i(\alpha_5) = \frac{E}{R} + (I_8 - \frac{E}{R})\, e^{-\frac{\alpha_5 - \beta_4}{Q_L}} \tag{3.2.18}$$

The output current waveform is computed over the interval from α_1 to α_5, starting with an assumed initial current of I_1 at α_1. The final value of output current at α_5, i.e., I_9 is compared

with I_1 for equality.Iterations are carried out till the initial and final currents I_1 and I_9 are equal. The steady state output current waveform is obtained for a particular modulation index and speed.

Having determined the steady-state output current waveform, the supply current waveform is calculated from the converter switching sequence. The input current waveform is Fourier analysed to get different harmonic contents. The performance characteristics are determined. The speed is changed in suitable steps to cover the entire range of speed. The modulation index is changed in steps of 0.1 and the above process is repeated.

The input performances are defined as follows :

Displacement Factor = $\cos(\tan^{-1}(a_1/b_1))$, where $a_1, a_2, \ldots, a_n$ and $b_1, b_2, b_3, \ldots, b_n$ are the Fourier coefficients of input line current waveform.

Distortion Factor = I_1/I_{srms},

where, I_1 = fundamental component of input line current

I_{srms} = rms input line current

Power Factor = Displacement Factor x Distortion Factor

Harmonic Factor = $(I_{srms}^2 - I_1^2)^{1/2} / I_1$

Ripple Factor = $(I_{rms}^2 - I_{av}^2)^{1/2} / I_{av}$

where, I_{rms} = rms value of output current

I_{av} = average value of output current

Efficiency of regeneration = Power returned to the supply/ machine power developed

Efficiency of motoring = Output power/Input power to the converter.

Fig. 3.2.1 shows the flow chart to determine these performance characteristics.

In what follows, the performance characteristics are explained for regenerating operation of the drive machine. Curves for motoring operation have also been shown. Curves in the first quadrant are for motoring and those in the fourth quadrant are for regeneration. In the regenerating operation, the dc separately excited drive machine acts as a generator and returns power to the three phase ac supply system through the three phase converter. The drive machine which is connected to a separately excited dc motor can be operated at any desired speed.

3.2.1 Speed Torque Characteristics

The speed torque characteristics are shown in Fig. 3.2.2. The armature current is mostly continuous because of multi-pulse width modulation. The speed regulation is quite good for a given modulation index. With a very low torque, does the speed regulation become poor owing to discontinuous conduction. The dotted curves show the boundary between the continuous and discontinuous conduction with the actual motor circuit parameters

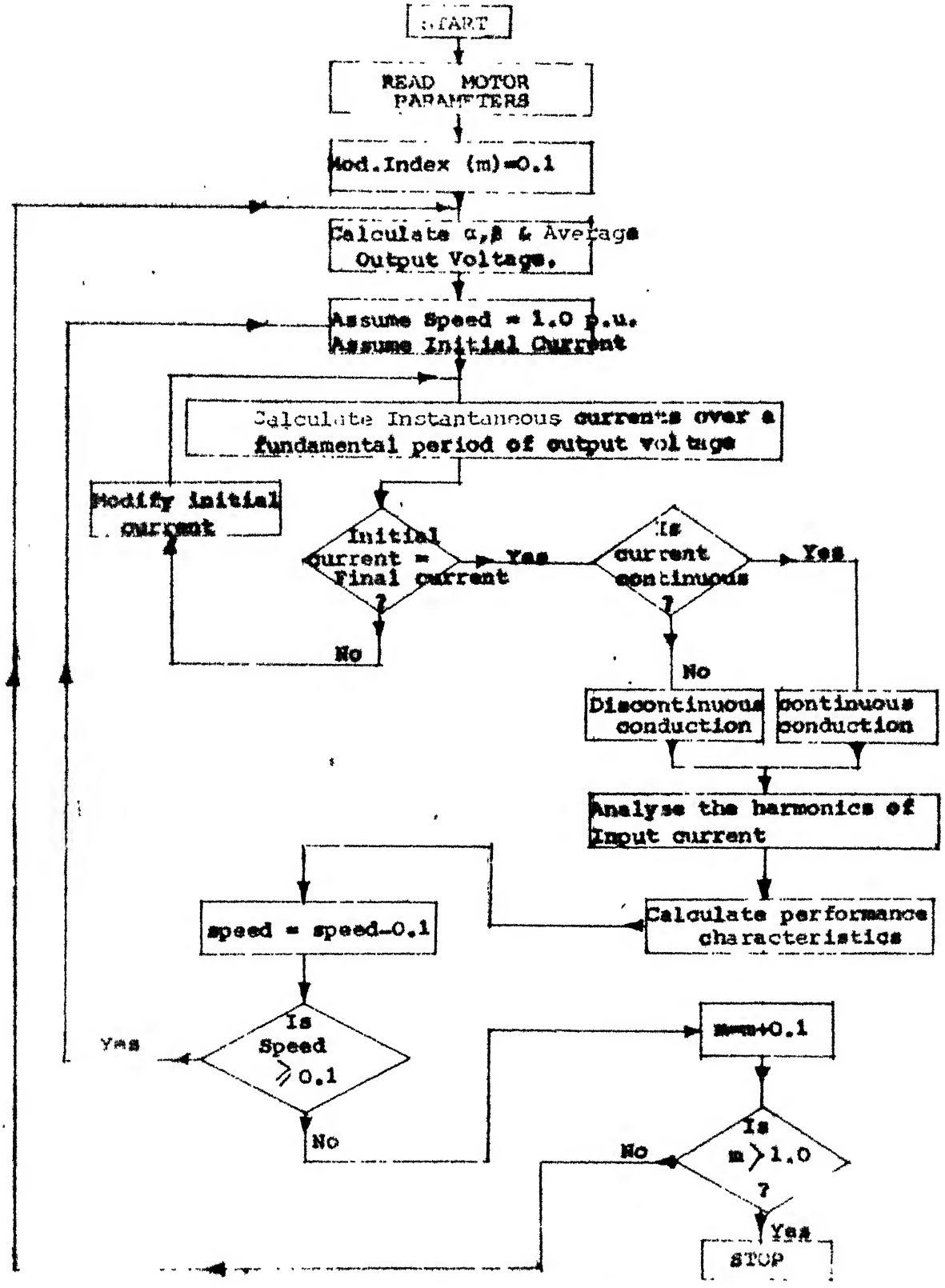

Fig. 3.2.1 Flow chart to determine the performance characteristics of a d.c. separately excited motor.

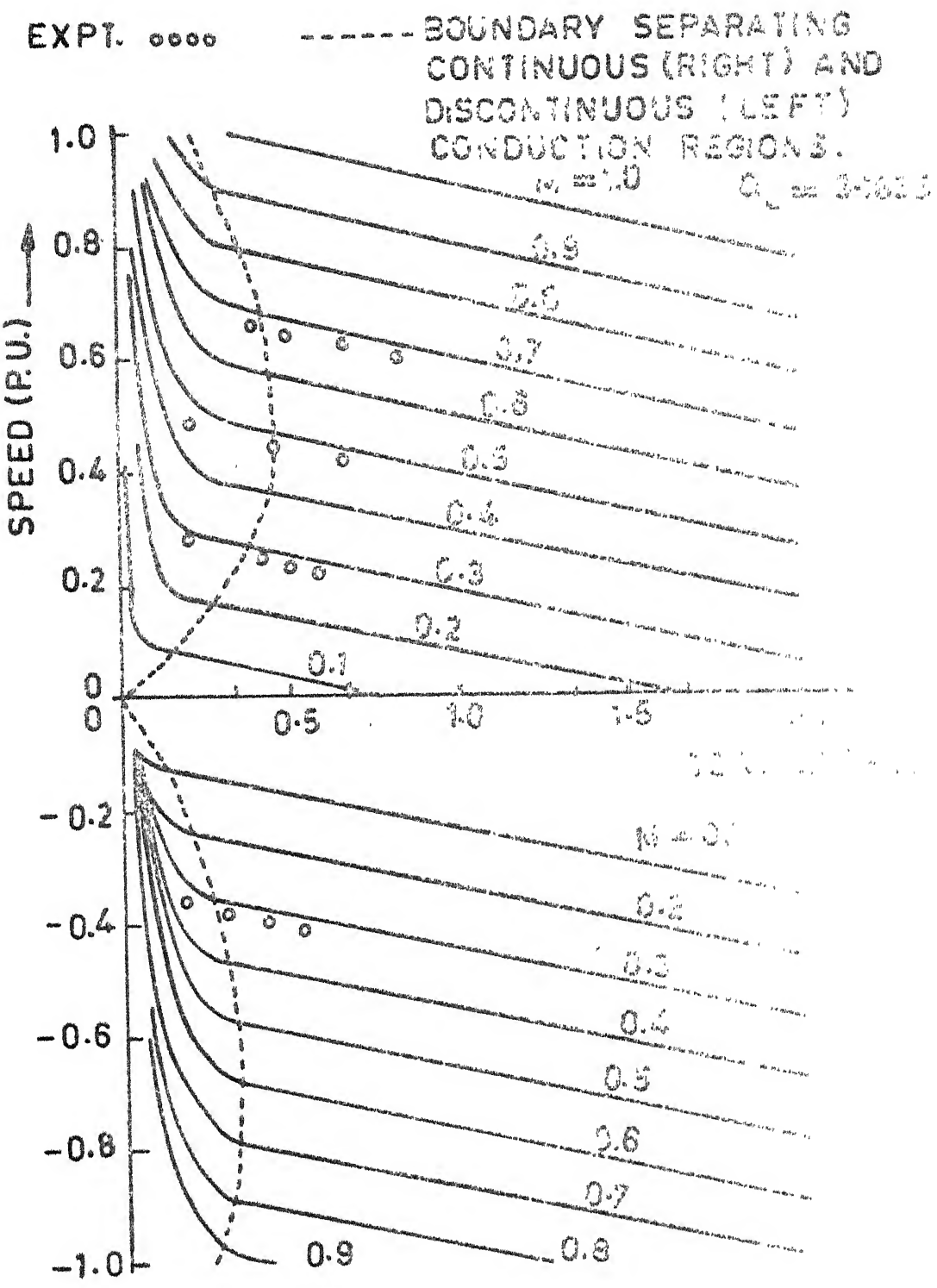

FIG. 3.2.2 SPEED TORQUE CHARACTERISTICS

The region of discontinuous conduction slightly deviates gradually from its linear nature. As the current becomes discontinuous in all pulses in one period of the output voltage for low torques, the speed regulation deteriorates considerably.

3.2.2 Displacement Factor and Power Factor

The displacement factor (Fig. 3.2.3) is unity for all values of modulation index in motoring and regenerating operation. Power factor increases with an increase in modulation index. For a given modulation index, the power factor is essentially constant. The range of speed over which the power factor is constant increases with an increase in modulation index in the motoring mode while it decreases in the regenerating mode. Both in motoring and regenerating operation the power factor for a particular modulation index tends to decrease as the current becomes discontinuous - at higher speed in case of motoring and at lower speed in case of regeneration.

3.2.3 Ripple Factor

The rms output current departs from the average current as the ripple factor increases with an increase in modulation index as shown in Fig. 3.2.4. In the case of motoring mode, the range of speed over which the ripple factor is constant increases with an increase in modulation index. However, it decreases in the case of regeneration. As the speed increases

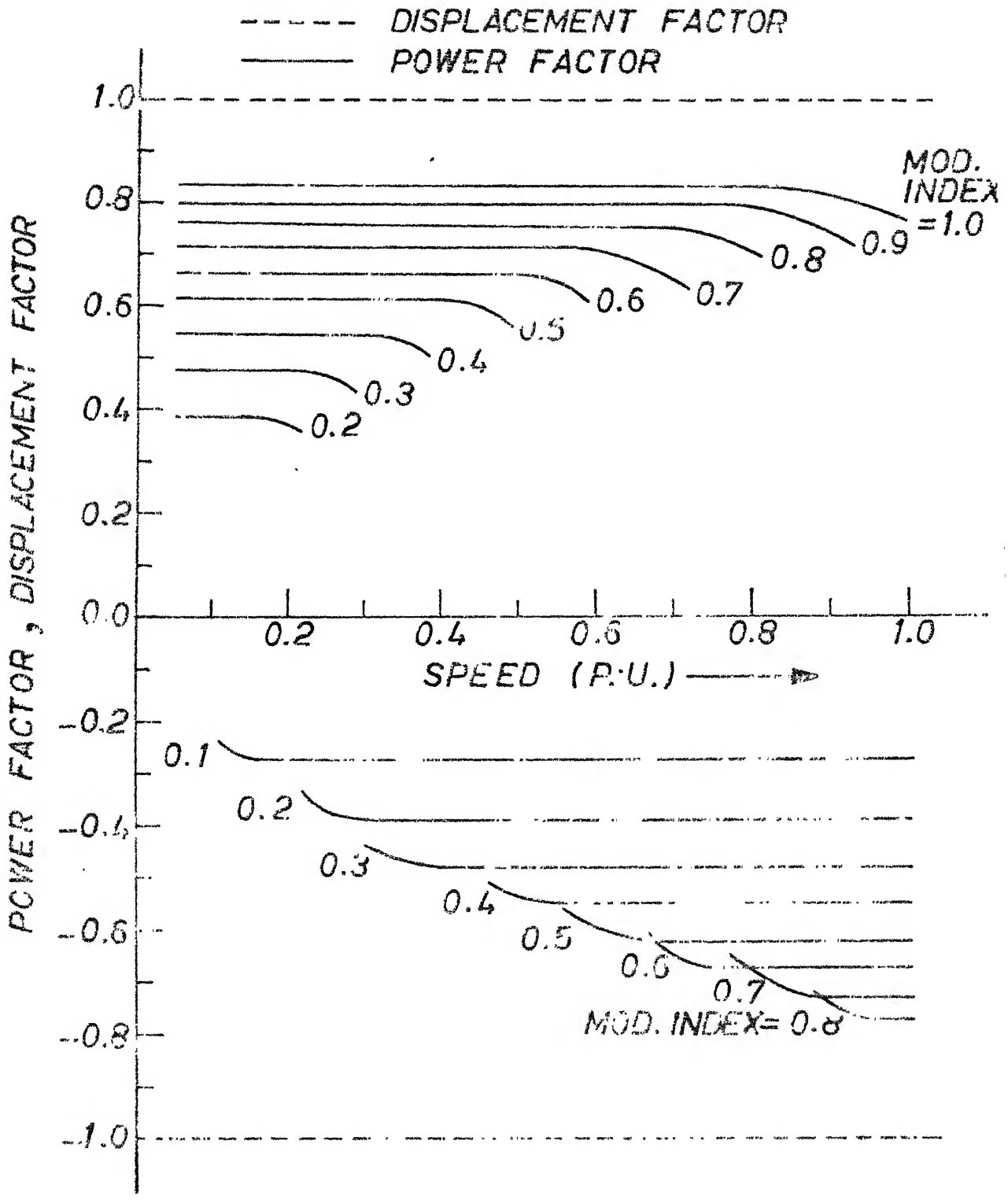

FIG. 3.2.3 VARIATION OF POWER FACTOR AND DISPLACEMENT FACTOR WITH SPEED FOR DIFFERENT VALUES OF MODULATION INDEX

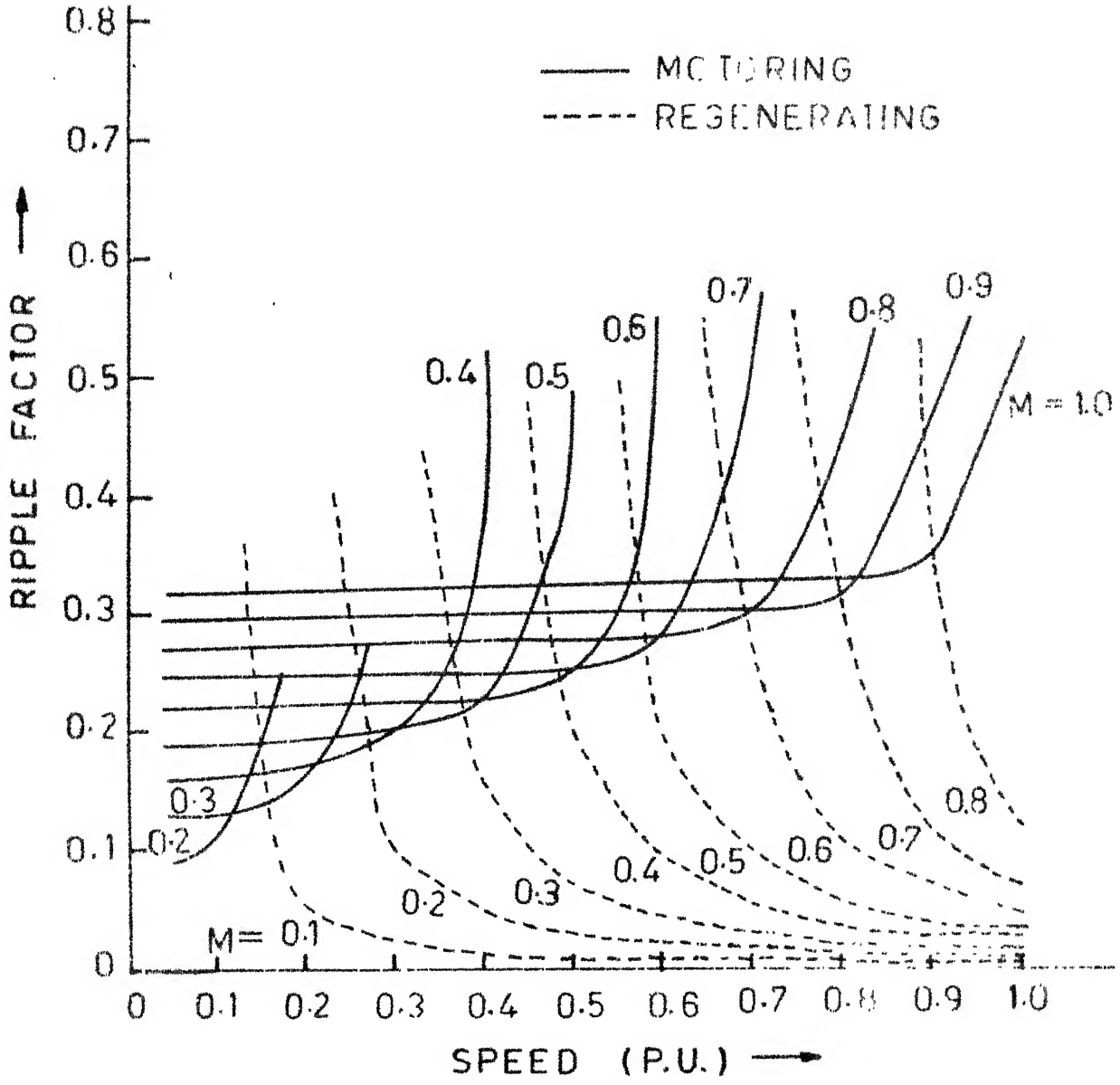

FIG 3.2.4 VARIATION OF RIPPLE FACTOR WITH SPEED FOR DIFFERENT VALUES OF MODULATION INDEX

beyond a certain value for a given modulation index, the ripple factor also increases significantly in case of motoring operation. In case of regeneration, for a particular modulation index, the ripple factor remains almost constant upto some speed but increases appreciably with a decrease in speed. For large values of modulation index, the ripple factor increases sharply with a decrease in speed.

3.2.4 Harmonic Factor

The harmonic factor is an index showing the amount of harmonic content generated in the supply lines. The harmonic factor (Fig. 3.2.5) decreases with an increase in modulation index. Only when the speed increases beyond certain value in the case of motoring mode and decreases beyond a particular value in the case of regeneration, for a particular modulation index, the harmonic factor increases due to discontinuous conduction. As the speed crosses these critical values, power factor decreases but the displacement factor remains constant at unity. Therefore, the fundamental component of source current decreases and the harmonic factor increases as illustrated in Fig. 3.25.

3.2.5 Peak Factor

The peak factor is important from the standpoint of machine commutation and thyristor ratings. The peak factor (Fig. 3.2.6) increases with an increase in speed for a

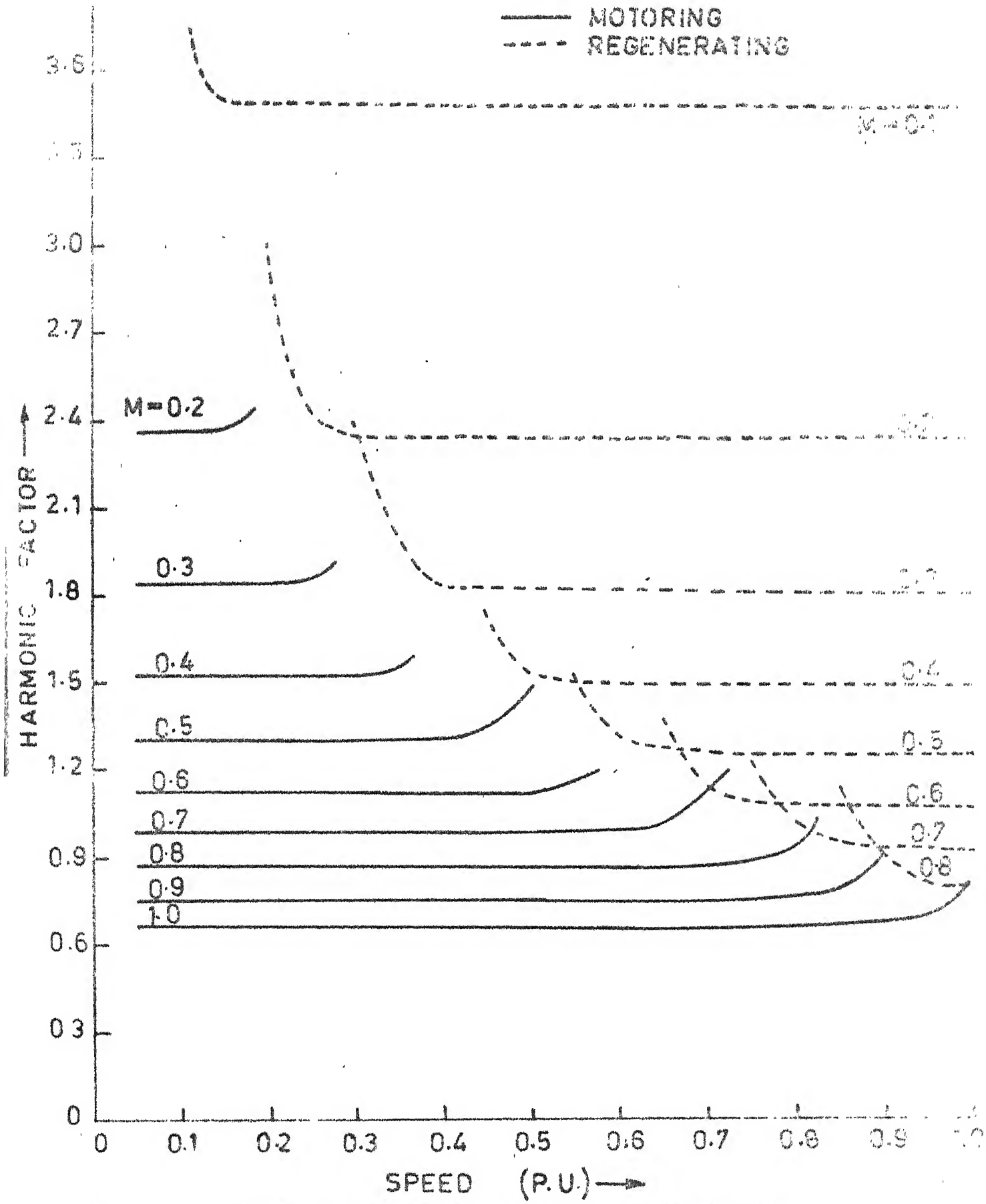

IG 3.2.5 VARIATION OF HARMONIC FACTOR WITH SPEED FOR DIFFERENT VALUES OF MODULATION INDEX

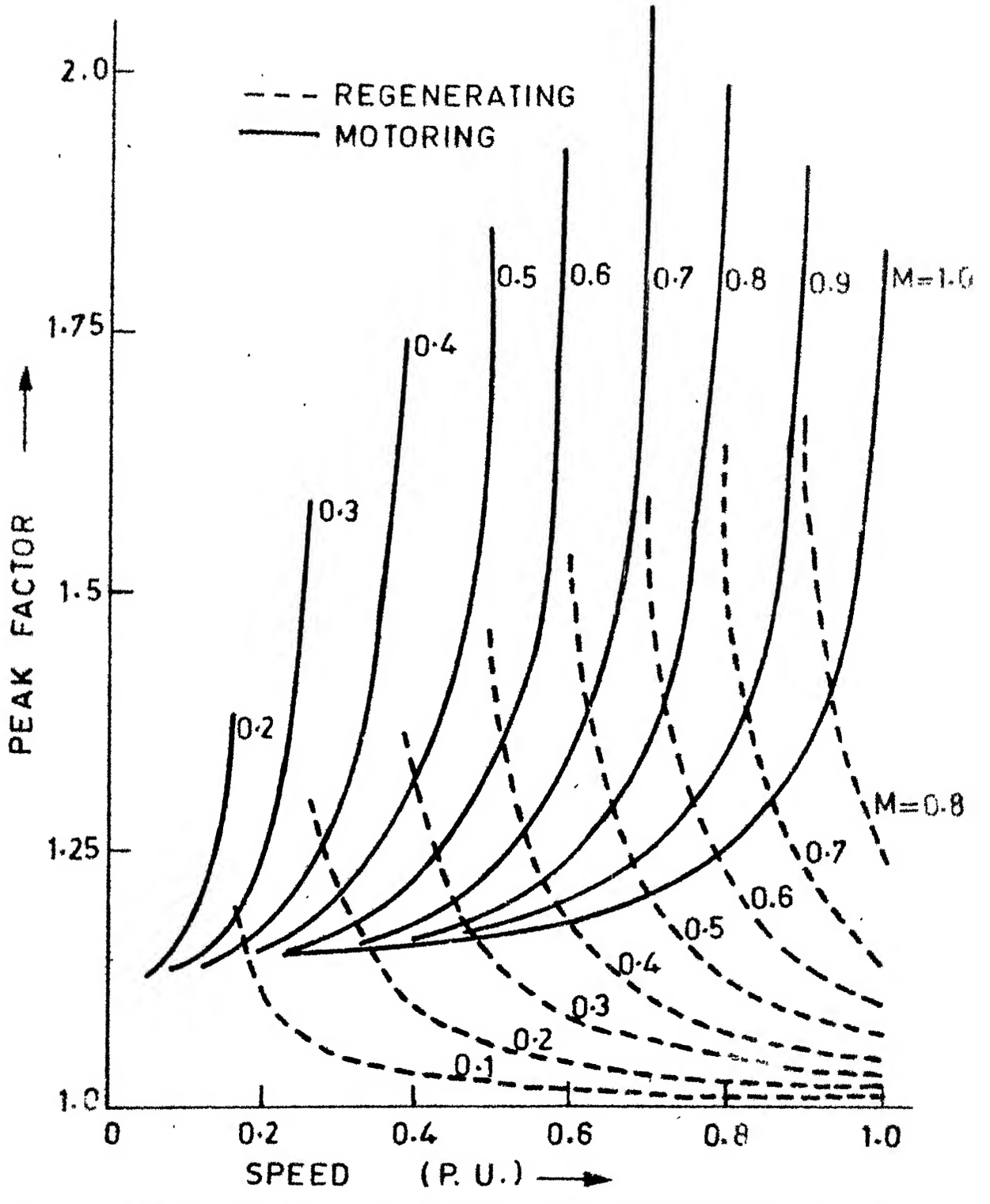

FIG 3.2.6 PEAK FACTOR VS SPEED FOR DIFFERENT VALUES OF MODULATION INDEX

particular modulation index in the case of motoring mode. At low speeds, the peak factor is low. The peak factor curves are terminated at different speeds for different modulation indices since the armature current becomes discontinuous beyond those speed-values. In the case of regeneration, the peak factor increases with a decrease in speed for a particular modulation index. For high speeds and small values of modulation index the peak factor is quite low and almost constant.

3.2.6 Efficiency

The curves showing the efficiency of motoring and regeneration are illustrated in Fig. 3.2.7 neglecting the no load loss of the motor. In the motoring mode, the efficiency increases with an increase in the speed for all values of modulation index. For a given speed of operation, the efficiency increases with a decrease in modulation index. The efficiency of regeneration increases with decrease in speed for a given modulation index. As the modulation index increases, the efficiency also increases. At higher speeds and smaller values of modulation index, the efficiency is quite low.

3.3 PERFORMANCE CHARACTERISTICS UNDER CONSTANT TORQUE OPERATION

Separately excited dc motors provide constant torque characteristics if the field current is maintained constant and

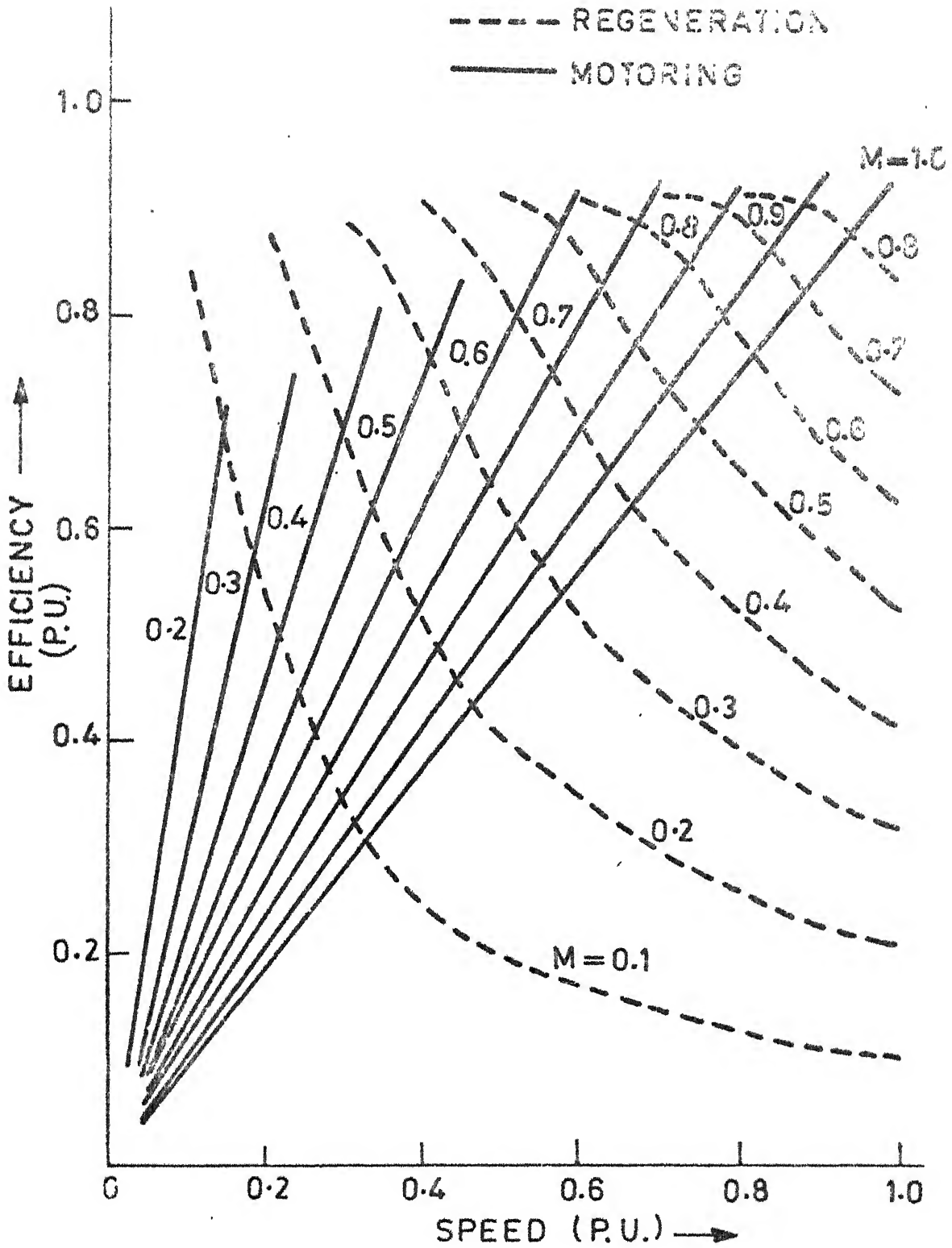

FIG. 3.2.7 EFFICIENCY VS. SPEED FOR DIFFERENT VALUES OF MODULATION INDEX

armature voltage is controlled [14]. The performance characteristics are studied under constant torque operation by digital simulation. In this case also, the commutation effects have been neglected and the converter circuit is assumed to operate with sinusoidal pulse width modulation (SPWM) control technique. To start with,the desired torque is set. For a given modulation index and an assumed speed, the equations given in Section 3.2 are solved and the average value of load current and hence the load torque are computed under steady-state conditions. The calculated torque and the set torque are compared. If the difference between these two torques is not below some tolerance, the speed is increased or decreased depending upon the calculated torque is higher or lower than the set torque. If the difference is within some tolerable limit, the instantaneous load current under steady-state is processed for determining the performance in the supply and the load as defined in Section 3.2. This procedure is repeated by changing the modulation index in Steps of 0.1. In what follows, the performance characteristics are presented for 100%, 75% and 50% of rated torque. Curves obtained for motoring mode are also shown alongwith those for regeneration.

3.3.1 Displacement Factor, Power Factor and Harmonic Factor

Fig. 3.3.1 shows the supply performance. The displacement factor is unity over the entire range of speed and load torques because of sinusoidal pulsewidth modulation. Since the displacement factor is unity, the power factor is also the same as distortion factor. The power factor increases with an increase in the speed. At a particular speed, in the case of motoring, the supply power factor is slightly improved with a higher load torque. This is consistent over the entire range of speed. The supply harmonic factor is quite low at high speeds. However, as the speed decreases, the harmonic factor increases appreciably. At a particular operating speed, the harmonic factor decreases with an increase in load torque. But the decrease is not very significant. At low speeds the power output is also low. Since the fundamental power factor is unity over the entire speed range, the fundamental component of supply current which contributes to the output power decreases significantly. This causes an increase in the harmonic factor as the speed is decreased.

Fig. 3.3.1(b) shows the supply performances when the drive system is operating under regeneration. Since the nature of these curves is almost the same as that for the motoring operation, the same explanation holds good in this

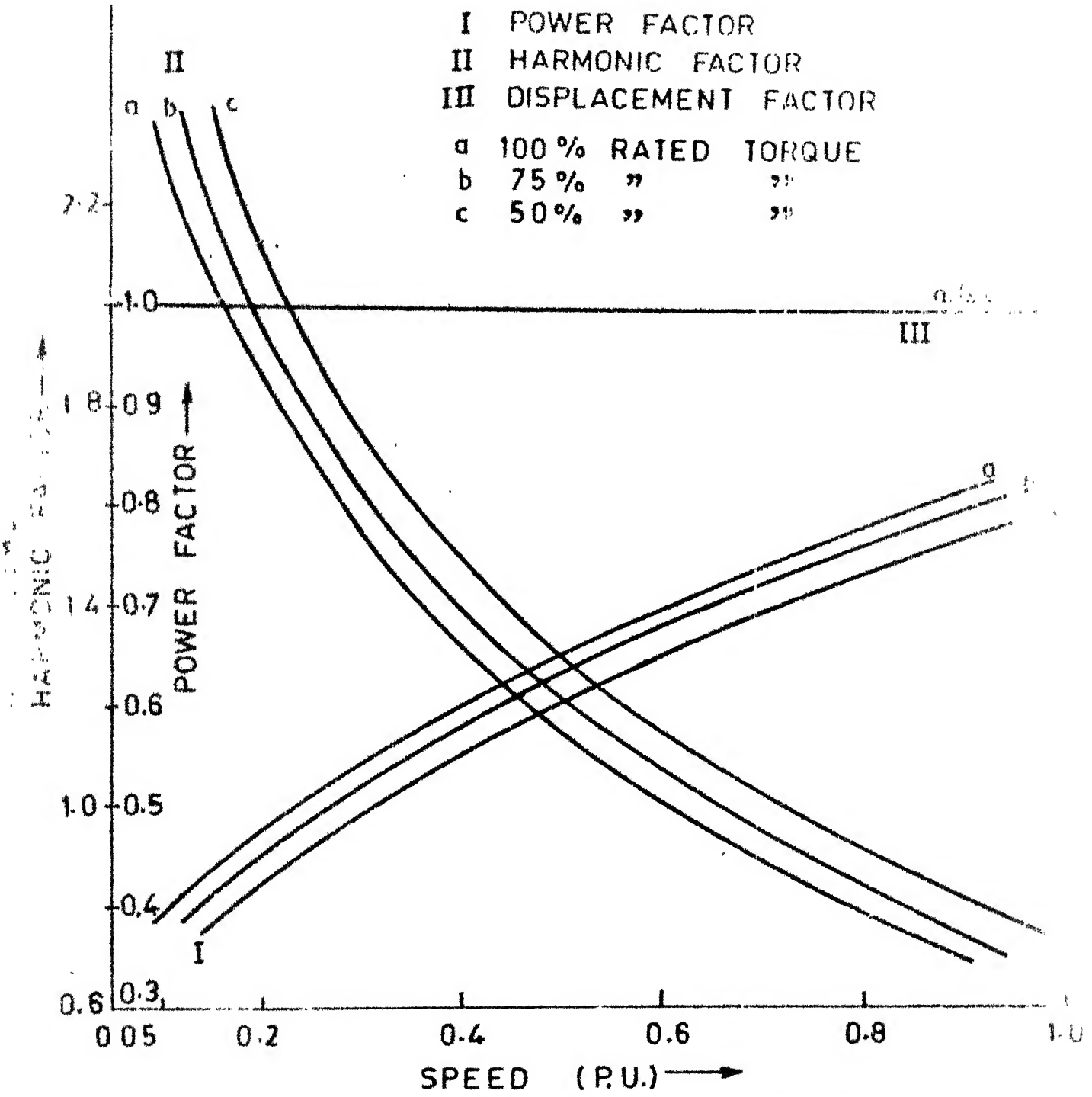

FIG: 3.3.1 (a) MOTORING OPERATION

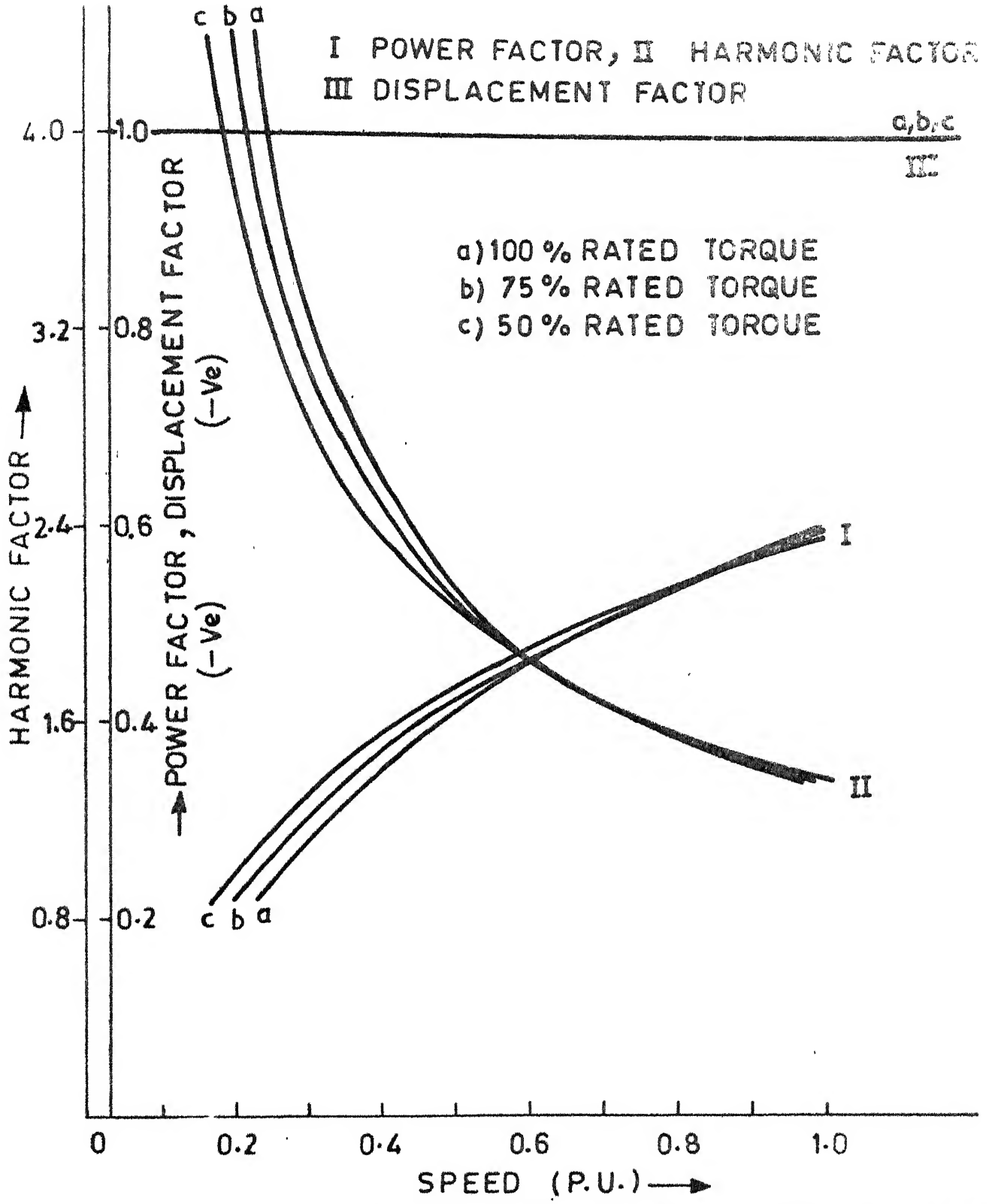

FIG 3.3.1 (b) POWER, HARMONIC & DISPLACEMENT FACTOR VS SPEED FOR CONSTANT TORQUE REGENERATING OPERATION

case also. In addition, at high speeds, the harmonic factor is the same for all load torques and the difference in the power factor is insignificant for all load torques.

3.3.2 Ripple Factor and Peak Factor

The ripple factor and peak factor are illustrated in Fig. 3.3.2(a) and (b) for motoring and regenerating mode respectively. Both the factors are lower in the latter operation. For both operation, the ripple factor increases with an increase in the speed. At a particular speed, the ripple factor increases with a decrease in load torque. The increase is quite pronounced for lower torques and in the higher speed range.

In the motoring mode, the peak factor increases appreciably with an increase in the speed, but decreases slightly with a further increase in the speed. At a particular speed, the peak factor increases with a decrease in load torque. The increase is quite pronounced at higher speeds and lower torques. In the regenerating operation, the peak factor increases with an increase in the speed. But remains almost constant with further increase in speed. For a particular speed, the peak factor increases with a decrease in the load torque, but increase is not significant as in motoring operation.

3.3.3 Supply Harmonic Spectrum

Fig. 3.3.3 illustrates dominant supply current harmonics for motoring and regeneration operations. Because of sinusoidal pulse width modulation with four pulses per half cycle, per phase, the harmonic spectrum has shifted from lower order to higher order frequency components. Because of three phase configuration, triplen harmonics are absent. The dominant harmonics are eleven and thirteen. They are quite significant at low speeds but decreases gradually as the speed increases. For a particular speed, the harmonics decrease slightly with an increase in the load torque. Other predominant harmonics in the order of their magnitude in the low frequency region are 5th, 7th, 4th and 2nd. These are of low amplitudes and their variations with speed and load torques are quite insignificant. Since, there is no half wave symmetry in the source current, even harmonics are also generated. Other higher order even harmonics such as 8th, 10th, 14th, 16th etc. are of relatively low amplitude and hence are not shown. 17th and 19th harmonics are also present but they are of low amplitude over the entire range of speed. The higher order harmonics, 23rd and 25th are quite significant at low speed but decrease as the speed increases. All these higher order harmonics are not shown in Fig. 3.3.3(a) and (b).

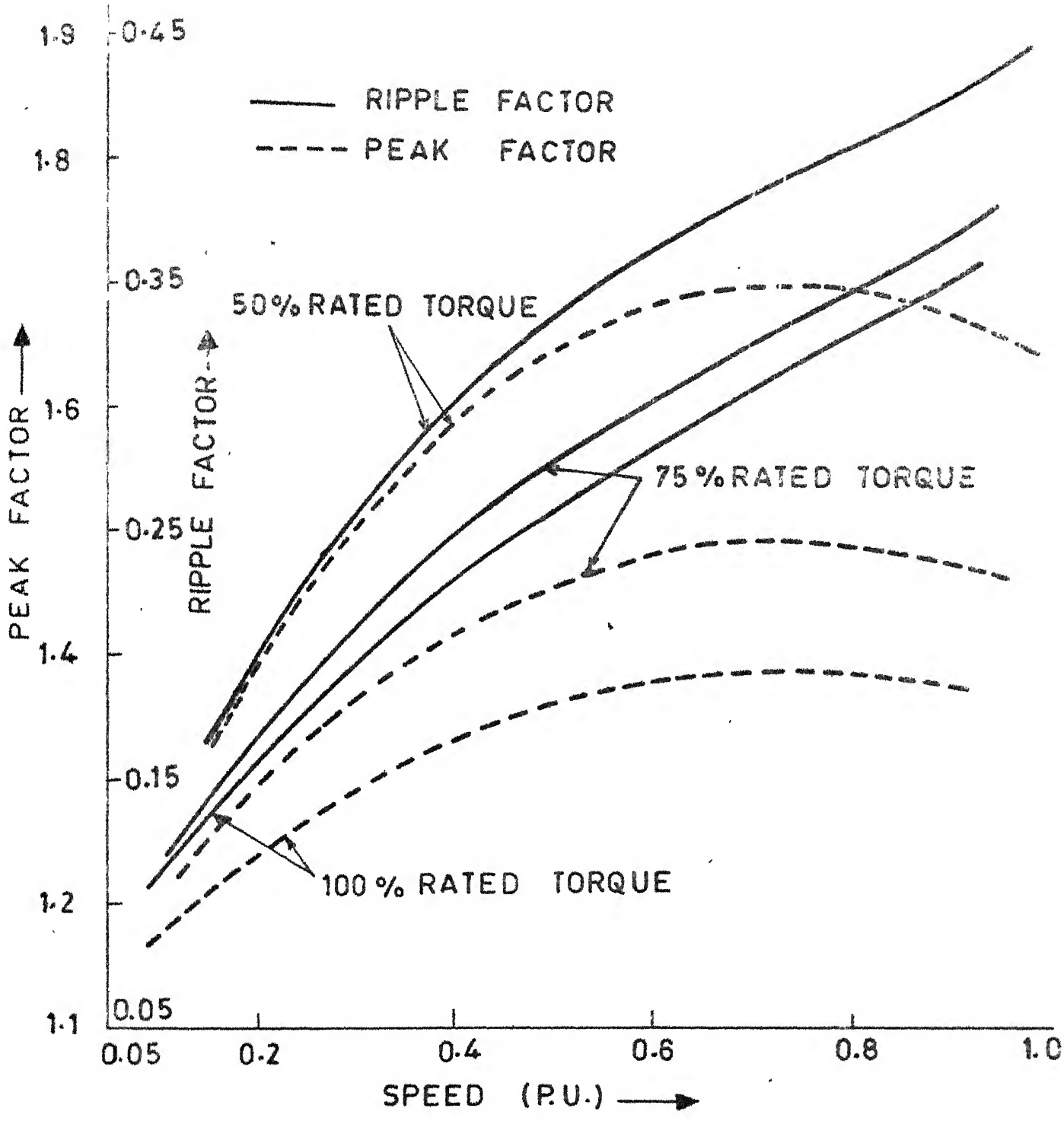

FIG. 3.3.2 (a) MOTORING OPERATION

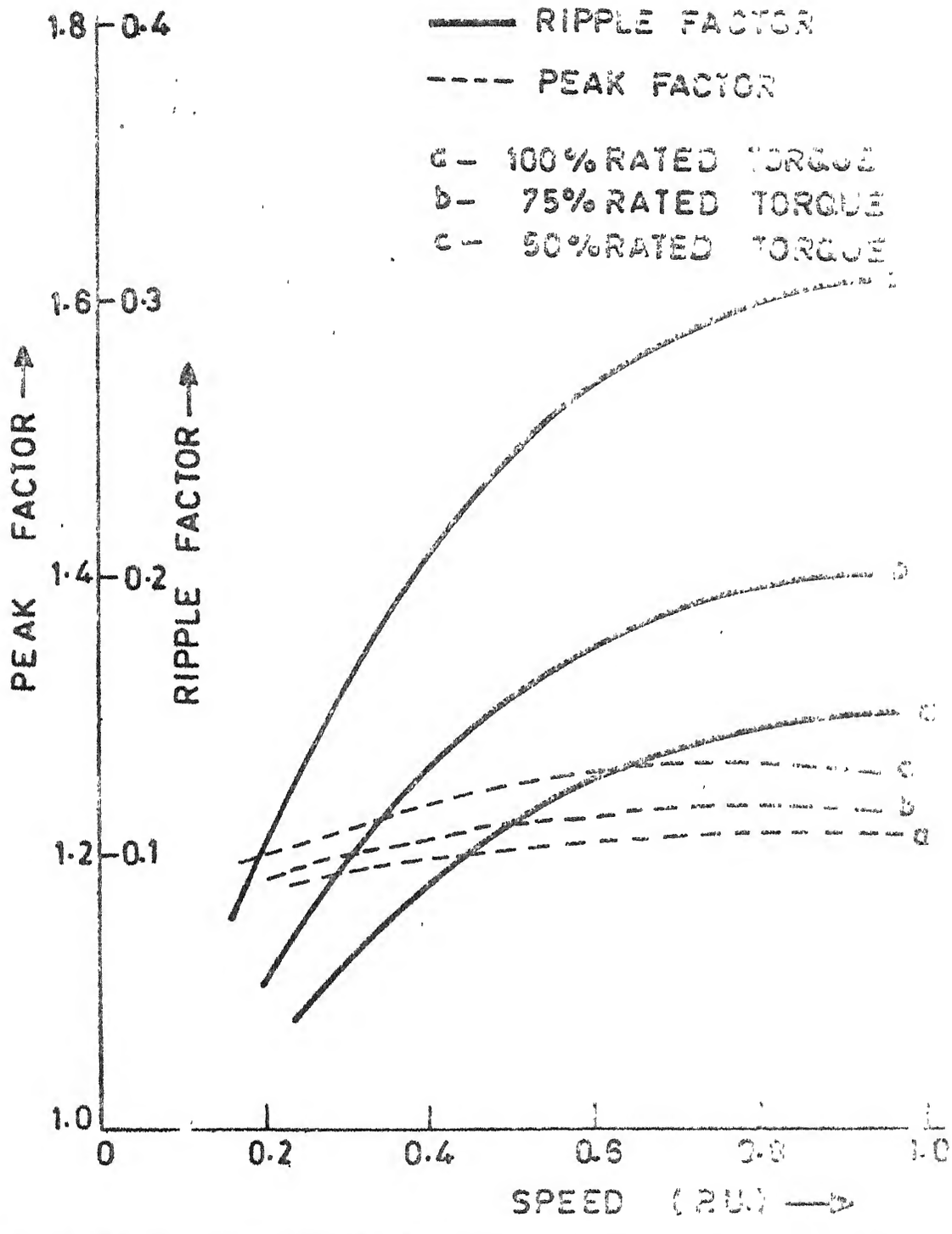

FIG 3.3.2 (b) VARIATION OF RIPPLE FACTOR AND PEAK FACTOR WITH SPEED FOR CONSTANT TORQUE REGENERATIVE OPERATION

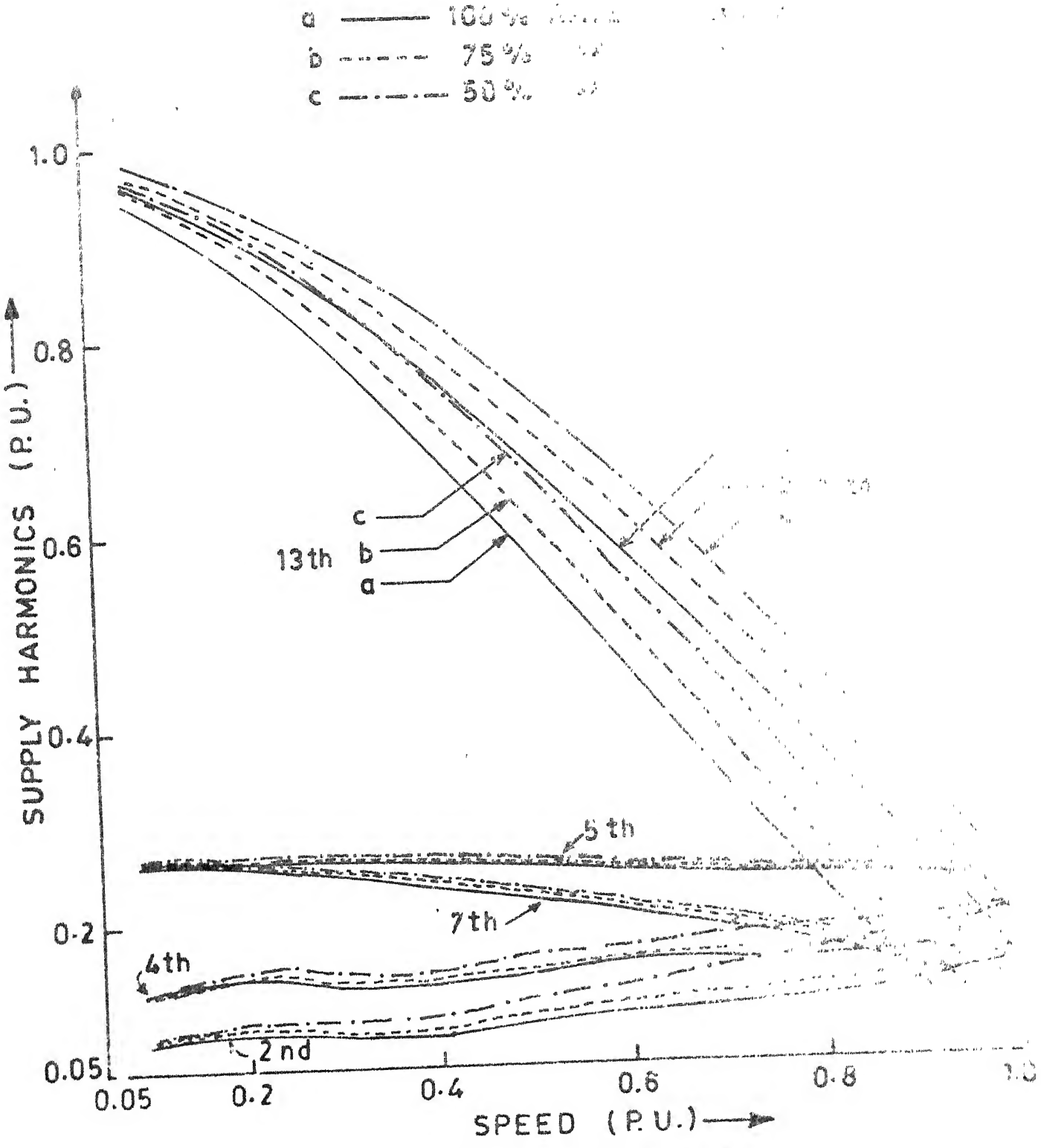

FIG 3.3.3 (a) MOTORING OPERATION

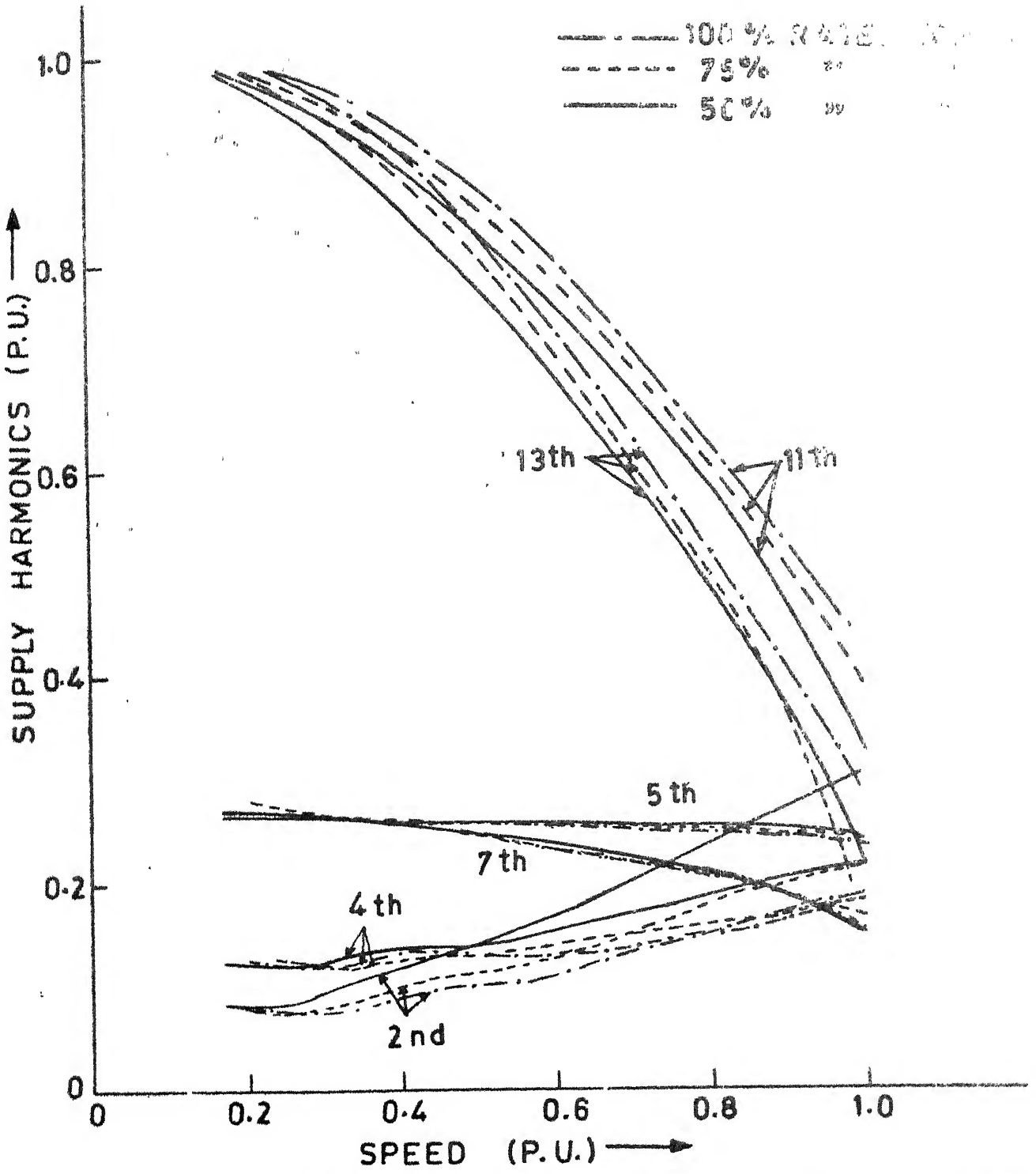

FIG 3 3.3 (b) VARIATION OF SUPPLY HARMONICS IN P.U. OF FUNDAMENTAL WITH SPEED FOR CONSTANT TORQUE REGENERATING OPERATION

3.4 DETAILED ANALYSIS OF THE CONVERTER

In this section, the analysis of the converter circuit is presented taking commutation effects also into account. Because of the presence of the thyristors and diodes, the converter circuit undergoes several topological modes. The switching devices are assumed to be ideal with zero resistance when conducting and infinite resistance when blocking. At any instant, the devices that are blocking are removed while those that are conducting are retained. State variables are assigned and a set of first order differential equations are written for the reduced converter circuit. Each topology of the converter circuit is recognised as a mode. The differential equations are then solved using the numerical method of Runge-Kutta Fourth Order. Approximation. The state variables are monitored and the mode change over is tested. If there is a change in the mode, a new set of differential equations is written for the incoming mode. The state variables computed at the end of a mode are fed as initial conditions if they continue to appear in the incoming mode. Those state variables which do not arise in the incoming mode are set zero. This is continued for one fundamental period which constitutes four pulses in this case. Under steady state condition, the initial value at the beginning of pulse 1 and final values at the end of pulse 4 must be the same. If there is a deviation between

the initial values and the final values, the initial values of state variables are modified and the process is repeated until the initial and final values are within some tolerable limits. After the steady state is reached, the time variation of different state variables are obtained for a desired operating point.

It is desired to establish the modes of operation of the converter circuit of Fig. 2.2.1 and to determine the sequence of modes for each pulse in the repetitive period of the output voltage in the steady-state. To start with, it is assumed that T_2,D_2 and T_5 are conducting the load current. At $\omega t = \alpha_1$, the thyristor T_1 is turned on. A reverse voltage is appeared across the thyristor T_2 due to the commutating capacitors and T_2 is turned off instantaneously. After deleting the nonconducting devices, the converter circuit is reduced to a simplified form which is designated as mode 1. The state variables chosen for the analysis and the derivation of first order differential equations are as follows :

$$x_1 = i_{D1}, \quad x_2 = i_{L1}, \quad x_3 = i_{L2}, \quad x_4 = i_D, \quad x_5 = v_{C1},$$

$$x_6 = v_{c2}, \quad x_7 = i_{L3} \qquad (3.4.1)$$

The devices conducting in mode 1 are given in Table 3.4.1. These devices are retained and the remaining devices are deleted from the circuit. The initial conditions at $t = t_o = \alpha_1/\omega$ are :

$$x_1(t_o) = 0, \quad x_2(t_o) = 0, \quad x_3(t_o) = 0, \quad x_4(t_o) = I_o,$$

$$x_5(t_o) = V_{CO}, \quad x_6(t_o) = V_{C2}, \quad x_7(t_o) = 0 \qquad (3.4.2)$$

The differential equations during this mode are obtained as follows :

$$\dot{x}_1 = 0 \qquad (3.4.3a), \qquad \dot{x}_2 = 0 \qquad (3.4.3b)$$

$$\dot{x}_7 = 0 \qquad (3.4.3c) \qquad \dot{x}_3 = (1/L_c)(x_5 - R_s x_3) \qquad (3.4.3d)$$

$$\dot{x}_4 = (1/L(x_5 - (R+2R_s)\ x_4 - E) \qquad (3.4.3e)$$

$$\dot{x}_5 = (-2/3C)(x_4 + x_3) \qquad (3.4.3f)$$

$$\dot{x}_6 = (1/3C)(i_d + i_{L2}) = (1/3C)(x_4 + x_3) \qquad (3.4.3g)$$

Equations (3.4.3(a)) to (3.4.3(g)) are integrated using Runge-Kutta 4th order approximation method. At the end of each step of integration, the mode changeover is checked by monitoring the capacitor voltage and the current i_{L2}. If capacitor voltage increases to the line voltage, v_{ab} faster than the current, i_{L2} dropping to zero, Mode 1 changes to Mode 2. Alternatively, if the current i_{L2} drops to zero first, Mode 1 changes to Mode 9. The state equations appropriate to the next mode are used for the testing of mode change over. The circuit configurations and the sets of state equations for all the possible modes are not given here. But from the Table 3.4.1 the topology for the various modes can be easily drawn. The condition

to be checked for a change in topology is also given for each mode. The mode sequence, thus obtained for the first four pulses for regenerating operation with a modulation index of 0.5 and at a speed of 310 rpm are shown in Fig. 3.4.1. Additional modes arising out of the commutations of the bottom group of thyristors are neglected in the present study.

Table 3.4.1

Topological modes of converter circuit of Fig 2.2.1
X: Device Conducting

Mode	T_1	T_2	T_3	D_{L1}	D_{L2}	D_{L3}	T_4	T_5	T_6	D_1	D_2	D_3	Test for Mode change over
1	X				X			X			X		$V_{C1} \leq V_{ab}$ → Mode 2 ; $i_{L2} = 0$ → Mode 9
2	X				X			X		X	X		$i_{D1} \geq i_d$ → Mode 3 ; $i_{L2} = 0$ → Mode 10
3	X				X			X		X			$i_{L2} = 0$ → Mode 4
4	X							X		X			wt = α_1 or α_2 → Mode 5
5		X		X				X		X			$i_{L1} = 0$ → Mode 6 ; $V_{C1} \geq V_{ab}$ → Mode 11
6		X						X		X			$V_{C1} \geq V_{ab}$ → Mode 7
7		X						X		X	X		$i_{D1} \leq 0$ → Mode 8
8		X						X			X		wt = α_2 or α_3 → Mode 13
9	X							X			X		$V_{C1} \leq V_{ab}$ → Mode 10
10	X							X		X	X		$i_{D1} \geq i_d$ → Mode 4
11		X		X				X		X	X		$i_{D1} \geq 0$ → Mode 12 ; $i_{Lb} = 0$ → Mode 7
12		X		X				X			X		$i_{L1} = 0$ → Mode 8
13	X				X				X			X	$i_{L2} = 0$ → Mode 14 ; $V_{C1} + V_{C2} \leq V_{ac}$ → Mode 16
14	X								X			X	$V_{C1} + V_{C2} \leq V_{ac}$ → Mode 15
15	X								X	X		X	$i_{D1} \geq i_d$ → Mode 18
16	X				X				X	X		X	$i_{L2} = 0$ → Mode 15 ; $i_{D1} > i_d$ → Mode 17
17	X				X				X	X			$i_{L2} = 0$ → Mode 18
18	X								X	X			wt = α_3 or α_4 → Mode 19
19			X	X					X	X			$i_{L1} = 0$ → Mode 20 ; $V_{C1} + V_{C2} \geq V_{ac}$ → Mode 23
20			X						X	X			$V_{C1} + V_{C2} \geq V_{ac}$ → Mode 21
21			X						X	X		X	$i_{D1} \leq 0$ → Mode 22
22			X						X			X	wt = α_4 → Mode 25 ; wt = α_5 → test steady state
23			X	X					X	X		X	$i_{L1} = 0$ → Mode 21 ; $i_{D1} \leq 0$ → Mode 24
24			X	X					X			X	$i_{L1} = 0$ → Mode 22
25	X						X		X			X	$V_{C1} + V_{C2} \leq V_{ac}$ → Mode 26 ; $i_{L3} = 0$ → Mode 14
26	X						X		X	X		X	$i_{D1} \geq i_d$ → Mode 27 ; $i_{L3} = 0$ → Mode 15
27	X						X		X	X			$i_{L3} = 0$ → Mode 18

CHAPTER IV

ERFORMANCE CHARACTERISTICS OF A DC SERIES FED FROM A THREE PHASE SPWM CONVERTER

ODUCTION

; series motors are extensively used in many applications. are particularly suited for applications that require high ting torque, such as cranes, hoists, elevators, vehicles :. Inherently,series motors can provide approximately onstant power output and are, therefore, particularly suited for traction drives. To obtain variable voltage dc for medium and large power dc series motors used in three-phase traction or in industrial drives as in cranes, special machine-tools,it is desirable to run the drive system through three-phase ac to dc converters.

The nonlinear variation of the induced emf with speed makes the analysis of the dc series motor more complex than that of a dc separately excited motor. The numerical solution [15] of the differential equations for all the modes of operation of a dc series motor demands considerable amount of computer time. To minimise computational time, certain approximate analytical methods of solution have been reported in the literature [16-17].

Franklin [16] described a method of analysis of a series motor fed by a current limit controlled dc-dc chopper wherein the magnetisation characteristic of the motor between the two current limits is approximated by a straight line. This method, however, can not be applied to the case of PWM converters where the limits between which the armature current fluctuates are not known beforehand. Dubey and Shepherd [17], described a method of analysis of dc series motor fed from a dc-dc chopper. This method suffers from two limitations : (i) it ignores instantaneous variation of armature induced emf due to the variation in field current and (ii) discontinuous conduction can not be predicted.

The method suggested by Krishnamurthy et al. [6] saves considerable amount of computer time without sacrificing the accuracy of computation. This method does not have the aforesaid limitations. The method has given satisfactory results with ac choppers and phase controlled converters. This strategy has been adopted in the present work to analyse the performance of a dc series motor driven from a three-phase SPWM ac-dc converter.

4.2 STEADY-STATE CURRENT EQUATIONS AND THEIR SOLUTION

Switching devices in the converter circuit have been assumed to be ideal. Commutation transients are neglected and resistance and self-inductance of the load circuit are assumed

to be constant. As the mechanical time constant of the motor is much higher than the converter switching time cycle, the fluctuation in the speed of the motor for a particular load can be neglected for all practical pruposes.

The mutual inductance, between the armature and the field of a series motor ($M_{af}(i)$), which is responsible for the induction of back emf in the armature circuit and which is a nonlinear function of the motor current i can be written as a fifth degree polynomial function of i [6],

$$M_{af}(i) = C_o + C_1 i + C_2 i^2 + C_3 i^3 + C_4 i^4 + C_5 i^5 \qquad (4.2.1)$$

The coefficients C_o to C_5 in eqn. (4.2.1) are obtained by fitting a fifth degree polynomial curve [18] into the magnetisation characteristics obtained experimentally. The curve fitting procedure is given in Appendix A.

Assuming M_{af} to be a function of average current rather than the instantaneous current and considering all average quantities, the motor equation can be written as

$$V_{dc} = M_{af}(I_{av})\ I_{av}.N + KN + I_{av}R \qquad (4.2.2)$$

where,

V_{dc} = average output voltage of the converter in Volts

N = speed of the motor in rad/sec.

K = constant for residual magnetism in Volts/(rad/sec.)

R = total motor circuit resistance in ohms.

At a particular modulation index, i.e., at a particular value of V_{dc} and with an assumed value of average output current, I_{av} the speed of the motor can be determined from equation (4.2.2).

During the interval $\alpha_1 \leq \omega t \leq \beta_1$ the equation of the motor circuit can be written as,

$$L \frac{di}{dt} + Ri + M_{af}(I_{av})\, i.N + KN = \sqrt{6}V \sin(\omega t+\pi/6) \qquad (4.2.3)$$

where, L = total inductance of the armature and the field of the motor in Henrys.

R = total motor armature circuit resistance including the field circuit in Ohms

V = rms supply voltage per phase (volts)

or $L \frac{di}{dt} + (R+M_{af}(I_{av})N)\, i + KN = \sqrt{6}\, V \sin(\omega t+\pi/6)$ ..

or $L \frac{di}{dt} + R'i + KN = \sqrt{6}V \sin(\omega t+\pi/6)$ (4.2.4)

where $R' = R+M_{af}(I_{av})\, N$

Solving this equation we get

$$i = \sqrt{\frac{6V}{Z}} \sin(\omega t+\pi/6-\phi') - \frac{KN}{R'} + A_1 e^{-\omega t/Q'_L} \qquad (4.2.5)$$

where

$$Z' = \omega^2 L^2+R'^2)^{1/2} \phi' = \tan^{-1} \frac{\omega L}{R'}$$

$$Q'_L = \frac{\omega L}{R'}$$

Let $i = I_1$ at $\omega t = \alpha_1$. Substituting this condition in eqn. (4.2.5),

$$i(\alpha_1) = I_1 = \frac{\sqrt{6}V}{Z'} \sin(\alpha_1+\pi/6-\phi') - \frac{KN}{R'} + A_1 e^{-\alpha_1/Q'_L}$$

Solving for A_1 and substituting for A_1 in eqn. (4.2.5), we get,

$$\text{or } i = \frac{\sqrt{6}V}{Z'} \sin(\omega t+\pi/6-\phi') - \frac{KN}{R'} + \left(I_1 - \frac{\sqrt{6}V}{Z'} \sin(\alpha_1+\pi/6-\phi') + \frac{KN}{R'}\right) \times e^{-\frac{\omega t-\alpha_1}{Q'_L}}$$

$$I_2 = i(\beta_1) = \frac{\sqrt{6}V}{Z} \sin(\beta_1+\pi/6-\phi') - \frac{KN}{R'} + \left(I_1 - \frac{\sqrt{6}V}{Z'} \sin(\alpha_1+\pi/6-\phi') + \frac{KN}{R'}\right) \times e^{-\frac{-\alpha_1}{Q'_L}} \qquad (4.2.7)$$

Similarly, current equations for different power and free-wheeling intervals are obtained as follows :

For $\beta_1 \leq \omega t \leq \alpha_2$

$$i = -\frac{KN}{R'} + \left(I_2 + \frac{KN}{R'}\right) e^{-\frac{\omega t-\beta_1}{Q'_L}} \qquad (4.2.8)$$

$$I_3 = i(\alpha_2) = -\frac{KN}{R'} + \left(I_2 + \frac{KN}{R'}\right) e^{-\frac{\alpha_2-\beta_1}{Q'_L}} \qquad (4.2.9)$$

For $\alpha_2 \leq \omega t \leq \beta_2$

$$i = \frac{\sqrt{6}V}{Z'} \sin(\omega t+\pi/6-\phi') - \frac{KN}{R'} + \left(I_3 - \frac{\sqrt{6}V}{Z'} \sin(\alpha_2+\pi/6-\phi') + \frac{KN}{R'}\right) e^{-\frac{\omega t-\alpha_2}{Q'_L}} \qquad (4.2.10)$$

$$I_4 = i(\beta_2) = \frac{\sqrt{6}V}{Z'} \sin(\beta_2+\pi/6-\phi') - \frac{KN}{R'} + \left(I_3 - \frac{\sqrt{6}V}{Z'} \sin(\alpha_2+\pi/6-\phi') + \frac{KN}{R'}\right) e^{-\frac{\beta_2-\alpha_2}{Q'_L}} \qquad (4.2.11)$$

For $\beta_2 \leq \omega t \leq \alpha_3$

$$i = -\frac{KN}{R'} + \left(I_4 + \frac{KN}{R'}\right) e^{-\frac{\omega t-\beta_2}{Q'_L}} \tag{4.2.12}$$

$$I_5 = -\frac{KN}{R'} + \left(I_4 + \frac{KN}{R'}\right) e^{-\frac{\alpha_3-\beta_2}{Q'_L}} \tag{4.2.13}$$

For $\alpha_3 \leq \omega t \leq \beta_3$

$$i = \sqrt{\frac{6V}{Z'}}\,(\omega t-\pi/6-\phi') - \frac{KN}{R'} + \left(I_5 - \sqrt{\frac{6V}{Z'}}\sin(\alpha_3-\pi/6-\phi') + \frac{KN}{R'}\right) \times e^{-\frac{\omega t-\alpha_3}{Q'_L}} \tag{4.2.14}$$

$$I_6 = i(\beta_3)$$

$$= \sqrt{\frac{6V}{Z'}}\,(\omega t-\pi/6-\phi') - \frac{KN}{R'} + \left(I_5 - \sqrt{\frac{6V}{Z'}}\sin(\alpha_3-\pi/6-\phi') + \frac{KN}{R'}\right) \times e^{-\frac{\beta_3-\alpha_3}{Q'_L}} \tag{4.2.15}$$

For $\beta_3 \leq \omega t \leq \alpha_4$

$$i = -\frac{KN}{R'} + \left(I_6 + \frac{KN}{R'}\right) e^{-\frac{\omega t-\beta_3}{Q'_L}} \tag{4.2.16}$$

$$I_7 = i(\alpha_4) = -\frac{KN}{R'} + \left(I_6 + \frac{KN}{R'}\right) e^{-\frac{\alpha_4-\beta_3}{Q'_L}} \tag{4.2.17}$$

For $\alpha_4 \leq \omega t \leq \beta_4$

$$i = \frac{\sqrt{6}V}{Z'} \sin(\omega t - \pi/6 - \phi') - \frac{KN}{R'} + \left(I_7 - \frac{\sqrt{6}V}{Z} \sin(\alpha_4 - \pi/6 - \phi') + \frac{KN}{R'}\right) e^{-\frac{\omega t - \alpha_4}{Q_L}} \quad (4.2.18)$$

$$I_8 = i(\beta_4)$$

$$= \frac{\sqrt{6}V}{Z'} \sin(\beta_4 - \pi/6 - \phi') - \frac{KN}{R'} + \left(I_7 - \frac{\sqrt{6}V}{Z'} \sin(\alpha_4 - \pi/6 - \phi') + \frac{KN}{R'}\right) e^{-\frac{\beta_4 - \alpha_4}{Q_L'}} \quad (4.2.19)$$

For $\beta_4 \leq \omega t \leq \alpha_5$

$$i = -\frac{KN}{R'} + \left(I_8 + \frac{KN}{R'}\right) e^{-\frac{\omega t - \beta_4}{Q_L'}} \quad (4.2.20)$$

$$I_9 = i(\alpha_5) = -\frac{KN}{R'} + \left(I_8 + \frac{KN}{R'}\right) e^{-\frac{\alpha_5 - \beta_4}{Q_L'}} \quad (4.2.21)$$

For steady-state condition $I_1 = I_9$.

4.3 COMPUTATION OF PERFORMANCE OF THE DC SERIES MOTOR

For a particular modulation index, the firing and extinction angles (α's and β's) are calculated and the average output voltage of the converter is determined using the equations given in Sec. 3.2. To start with, an arbitrary value is assumed for the average load current. The speed of operation is calculated

from equation (4.2.2). With an assumed initial value of I_1, the currents I_2 to I_9 are determined using the equations given in Section 4.2. In the computer simulation, the value I_9 is compared with I_1. If the absolute difference is not within a certain tolerable, limit, the computation is continued with a new value of I_1 which is equal to I_9. The procedure is continued until steady-state has been reached. After the steady state is obtained, the steady state current waveform is analysed to obtain different performance characteristics as defined in Sec. 3.2 This procedure is repeated for other values of average current to cover the entire range of current and speed. The modulation index is changed and the procedure is repeated. The flow-chart of Fig. 4.3.1 illustrates the procedure for computing the performance characteristics of a dc series motor.

4.3.1 Speed Torque Characteristics

The speed-torque characteristics are shown in Fig. 4.3.2. Nature of these curves are like the normal speed-torque characteristic of a dc series motor which gives high torque at low speed and low torque at high speed. The curves show continuous conduction within the operating range of the speed. In a series motor, the back emf is proportional to the motor current if the speed is assumed constant and if the nonlinearity in the magnetisation characteristic is neglected. This gives rise to

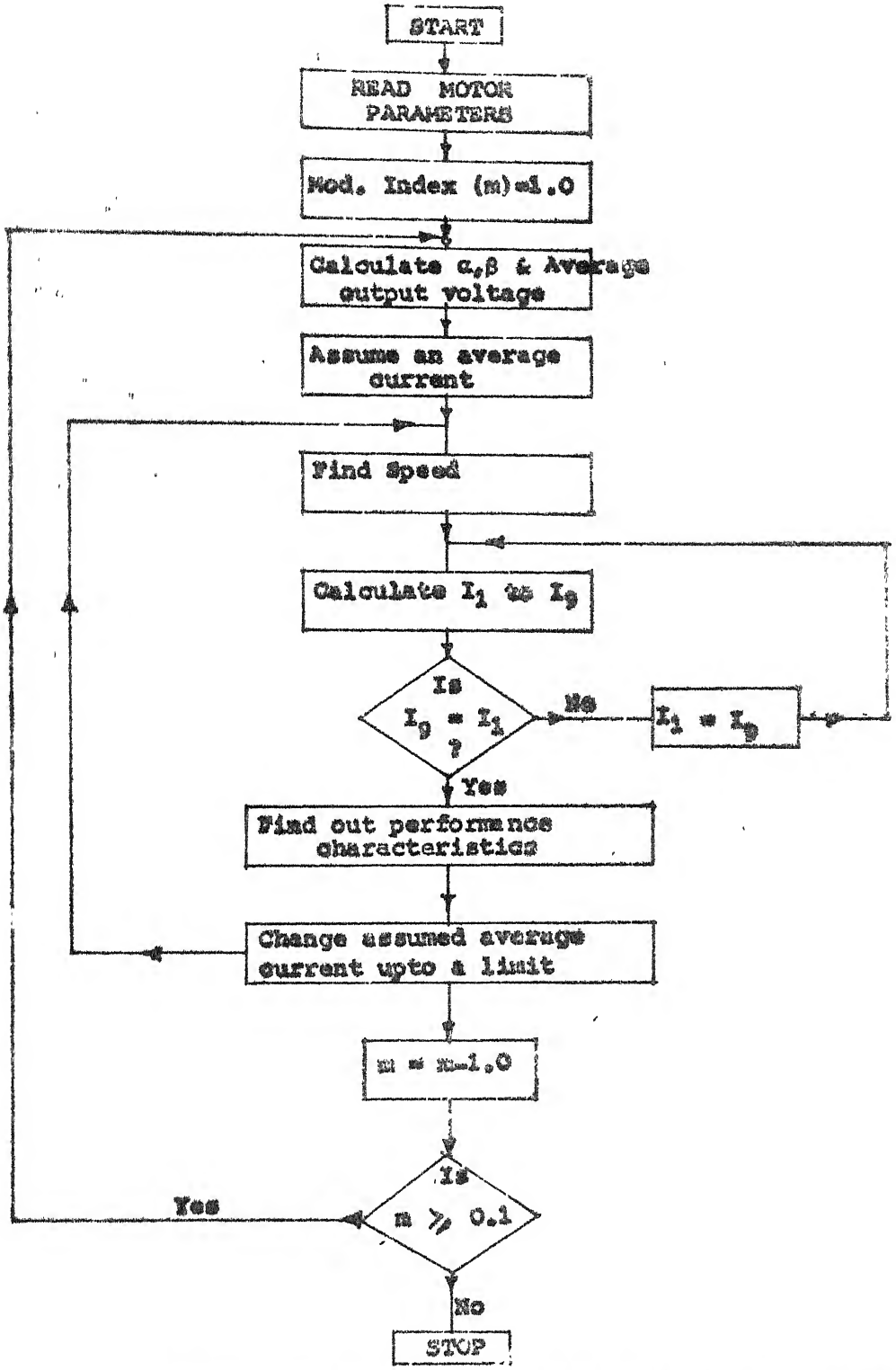

Fig. 4.3.1 Flow chart for obtaining the performance characteristics of a d.c. series motor.

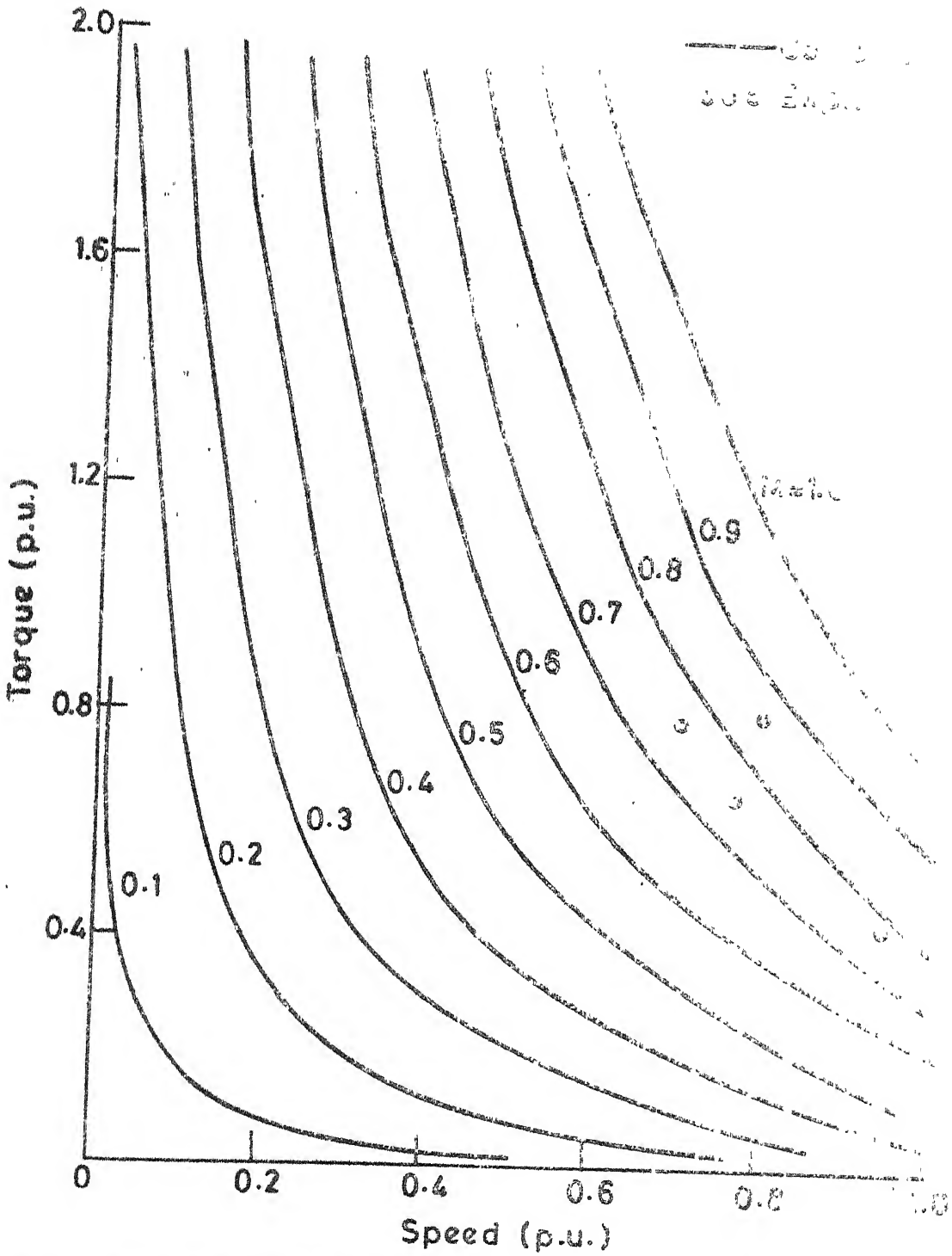

G. 4.3.2 SPEED-TORQUE CHARACTERESTICS OF A THREE PHASE AC-DC CONVERTER-FED DC SERIES MOTOR

continuous conduction over a wide range of speed. At very high speeds, of course, the current becomes discontinuous. If an additional inductance is inserted - in series with the motor armature terminals, the current becomes continuous over a wide range of speed of operation. Experimental values as shown in Fig. 4.3.2 closely follow the curves obtained theoretically.

4.3.2 Displacement Factor and Power Factor

The displacement factor (Fig. 4.3.3) is unity for all values of modulation index. The power factor increases with an increase in the modulation index. For a given modulation index the power factor is almost constant as in the case of a separately excited motor. At lower values of modulation index the power factor curves droop slightly as the speed is increased. This may be attributed to the distortion of the input current at higher speeds.

4.3.3 Ripple Factor

Ripple factor (Fig. 4.3.4) gives an idea of the deviation of rms output current from the average current. In contrary to the case of a separately excited motor the ripple factor decreases with an increase in the modulation index. At higher values of torque i.e., at lower values of speed the variation of ripple factor with speed is not significant.

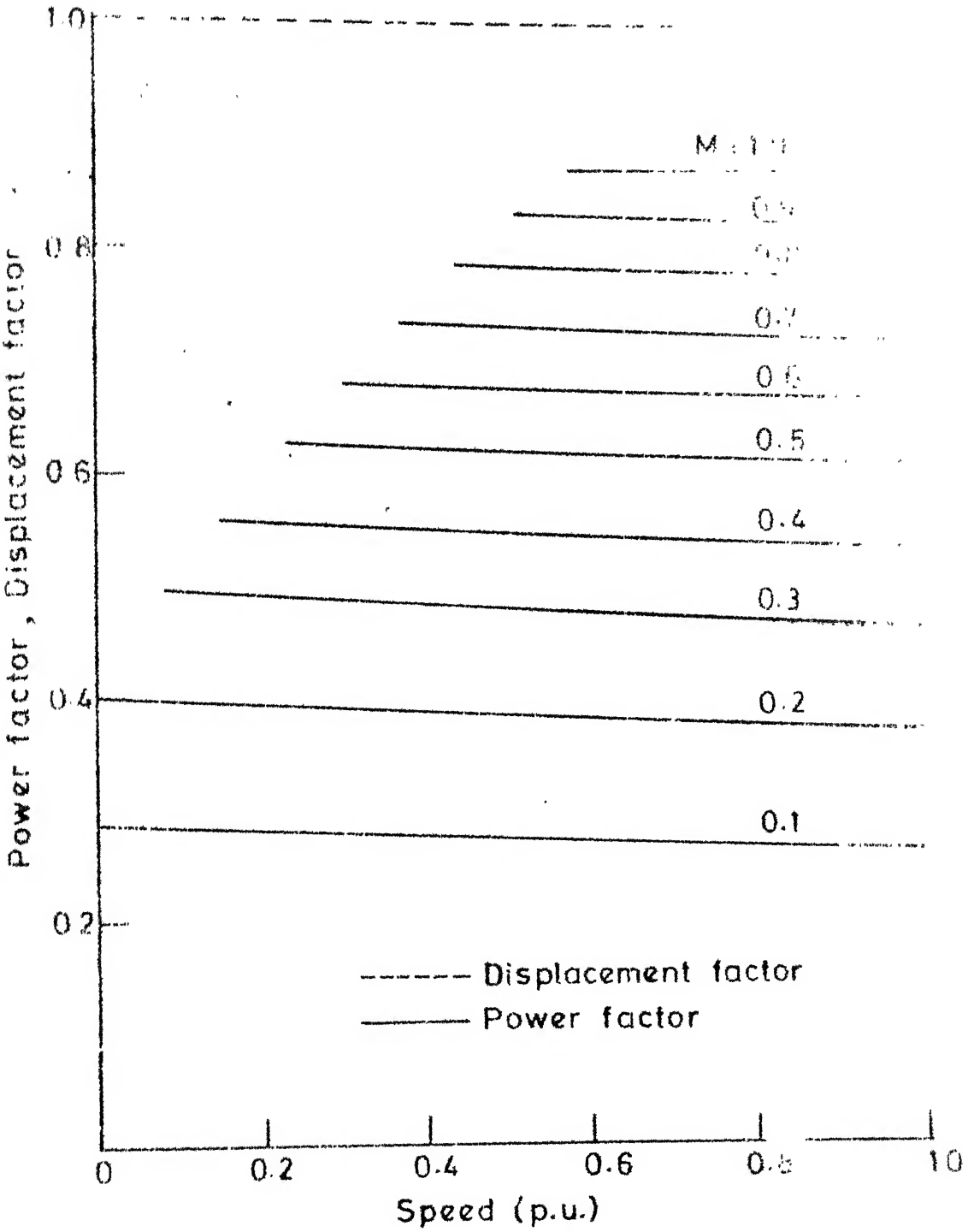

6.4.3 VARIATION OF DISPLACEMENT FACTOR AND POWER FACTOR WITH SPEED FOR DIFFERENT VALUES OF MODULATION INDEX

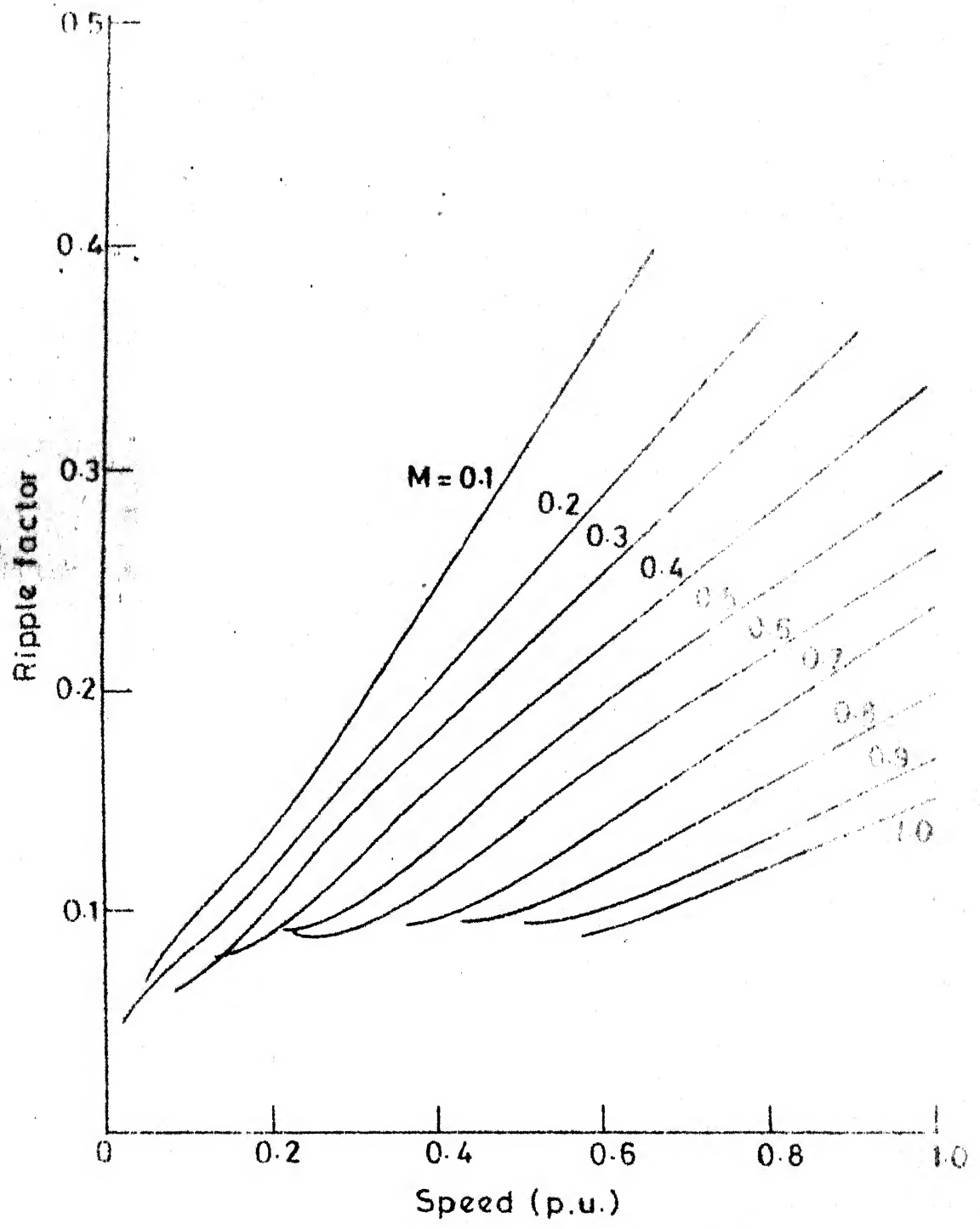

FIG. 4.3.4 RIPPLE FACTOR VS. SPEED FOR DIFFERENT MODULATION INDEXES

4.3.4 Harmonic Factor

At higher values of modulation index, the harmonic factor (Fig. 4.3.5) remains essentially constant as the speed is varied. At lower values of modulation index, the harmonic factor increases slightly, with an increase in the speed. At a particular value of operating speed the harmonic factor decreases significantly when the modulation index is increased.

4.3.5 Peak Factor

The peak factor curves (Fig. 4.3.6), as expected, follow the same nature of variation as that of the ripple factor. Peak factors as determined from experimental results at different speeds with modulation indices 0.9 and 0.3 are also shown in Fig. 4.3.6. These experimental values closely conform to the computed results.

4.4 PERFORMANCE CHARACTERISTICS UNDER CONSTANT POWER OPERATION

The torque-speed characteristics of the ac-dc PWM converter-dc series motor are such as to introduce high torque at low speeds, and low torque at high speeds. DC series motors are often used for constant power operation. The speed-torque curves shown in Fig. 4.3.2 do not conform to constant power, over the entire range of speed. To obtain a constant horsepower operation, the modulation index has to be changed to have different operating speeds.

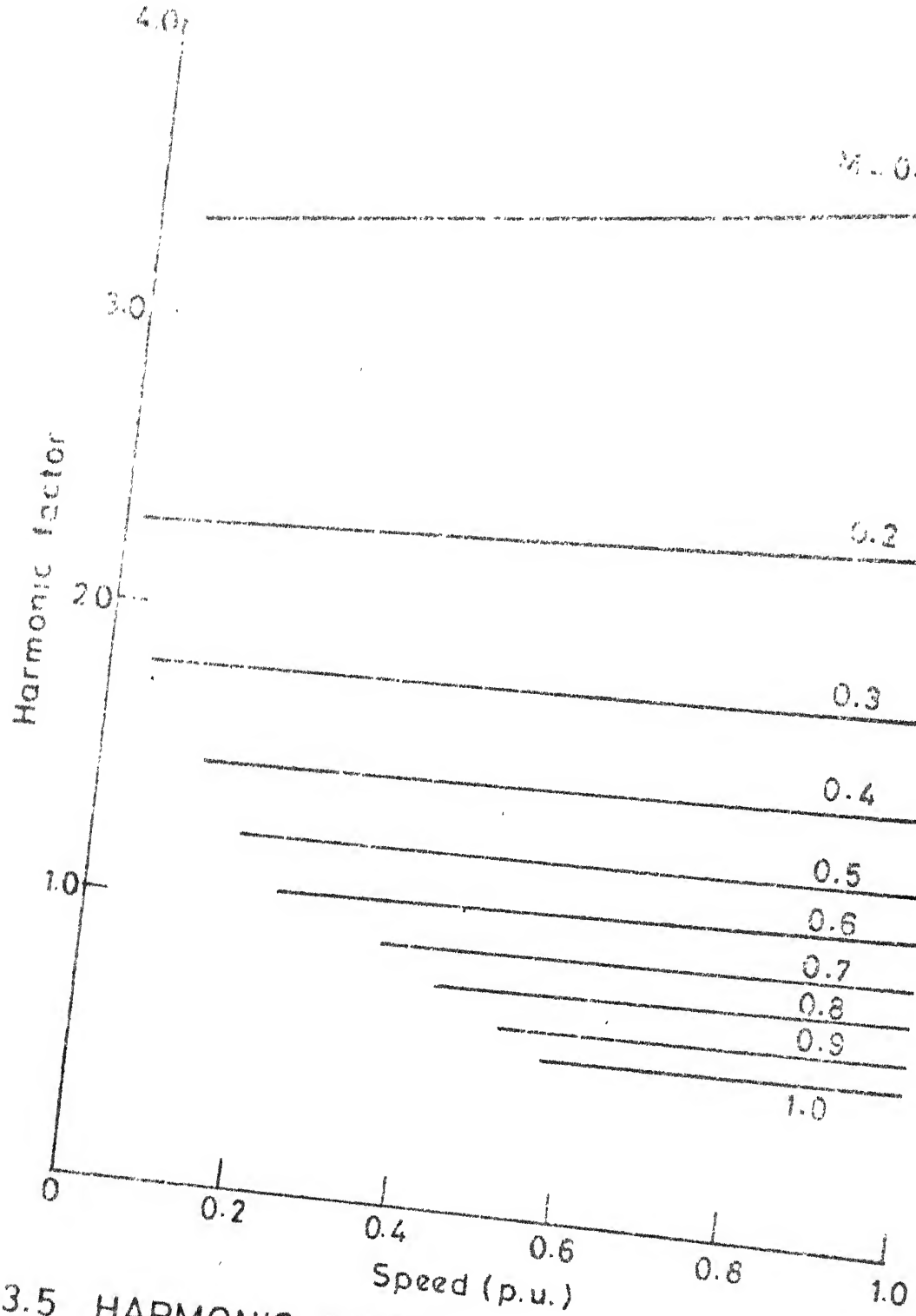

FIG. 4.3.5 HARMONIC FACTOR VS. SPEED FOR DIFFERENT VALUES OF MODULATION INDEXES

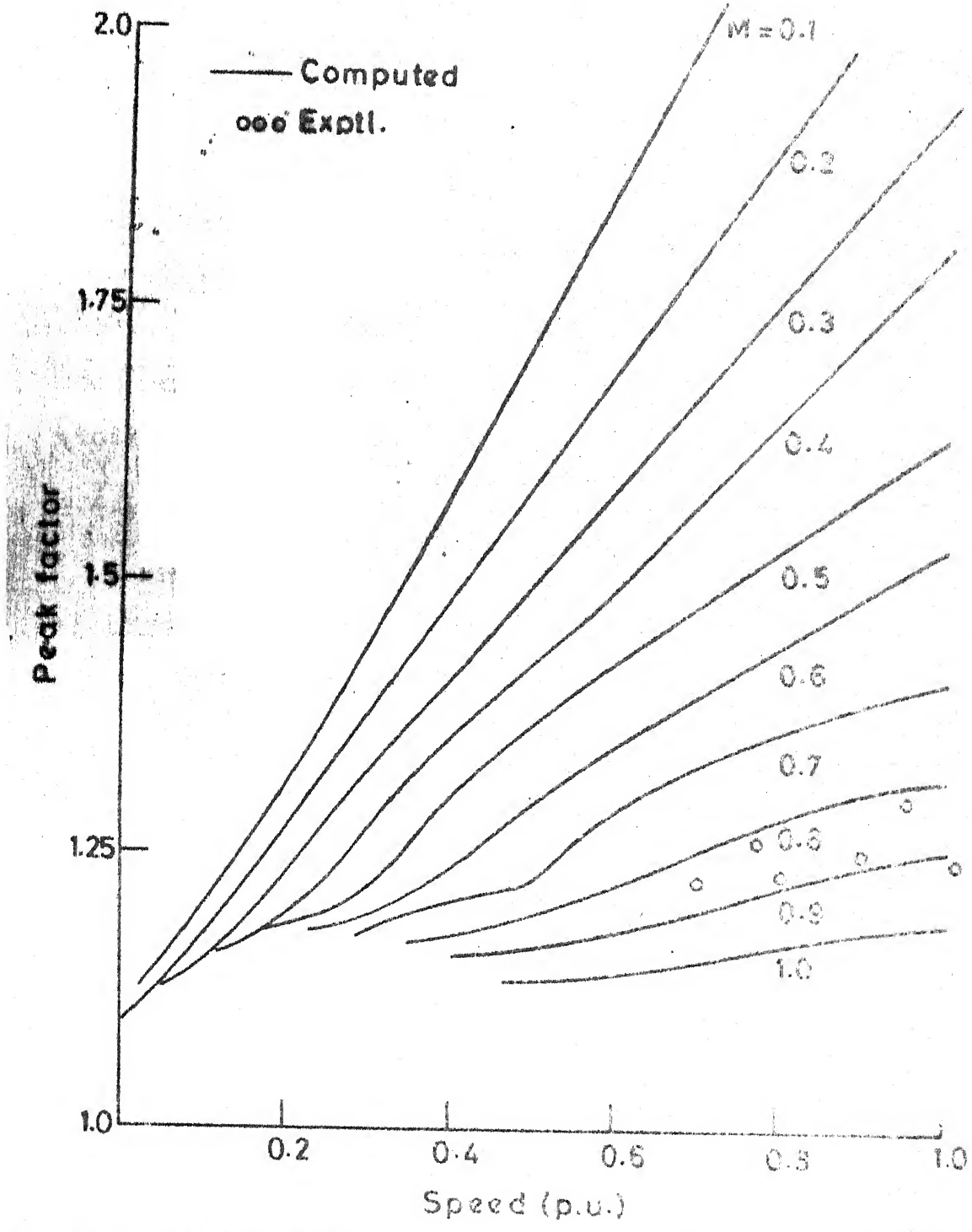

FIG. 4.3.6 PEAK FACTOR VS. SPEED FOR DIFFERENT VALUES OF MODULATION INDEX

The performance characteristics are obtained by neglecting the commutation transients and assuming that the converter circuit operates with the SPWM control technique. The flow-chart for determining the performance under constant torque operation is shown in Fig. 4.4.1. Results are obtained with three levels of power viz., 100%, 75% and 50% of nominal HP. Performance characteristics thus obtained are described in the sections that follow.

4.4.1 Displacement Factor, Power Factor and Harmonic Factor

Fig. 4.4.2 shows the supply performance. The displacement factor is unity over the entire range of speed and output power because of sinusoidal pulse width modulation. The power factor, for a particular constant output power, increases with an increase in the speed. The peak factor increases with an increase in the output power-level over the entire range of speed. The supply harmonic factor is low at high speeds and power outputs. It increases with a reduction in speed for all power levels. Also, the harmonic factor decreases when the operating power is increased for a particular speed. The difference in harmonic factor at various speeds for two different levels of power remains practically the same throughout the entire speed range.

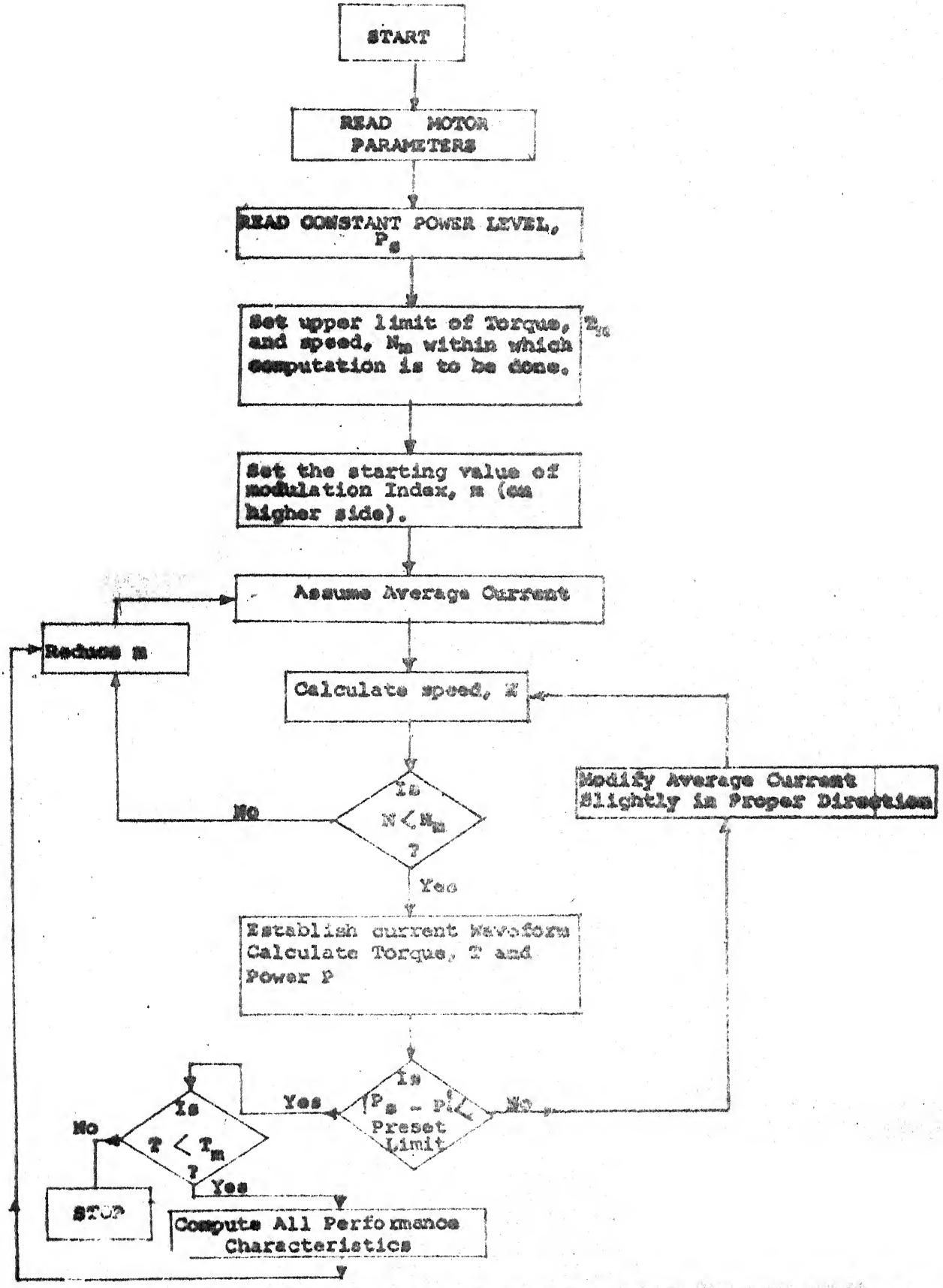

Fig. 4.4.1 Flow chart to determine the performance characteristics under constant power operation.

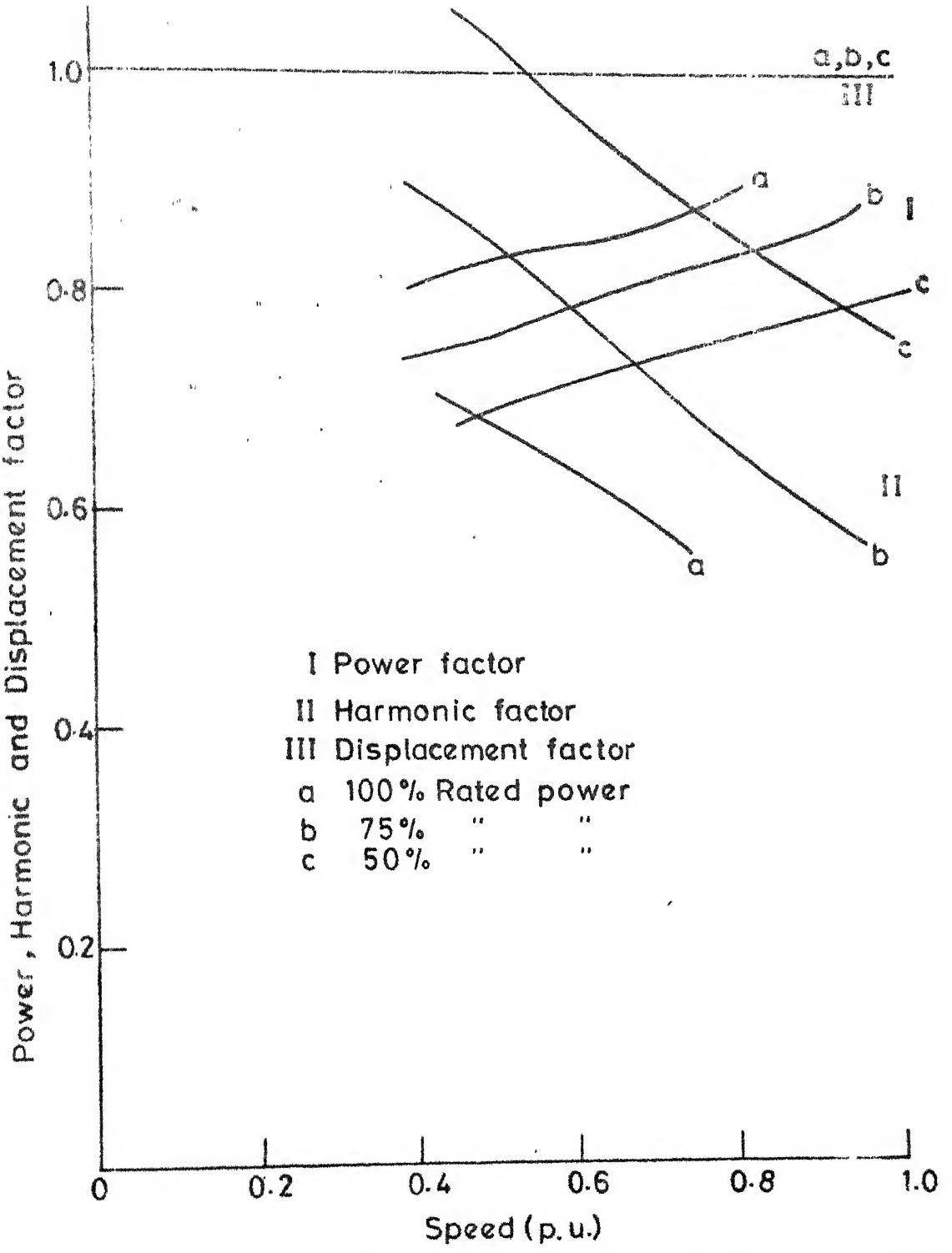

FIG. 4.4.2 VARIATION OF POWER, HARMONIC AND DISPLACEMENT FACTOR WITH SPEED FOR CONSTANT POWER OPERATION.

4.4.2 Ripple Factor and Peak Factor

The ripple factor and peak factor are illustrated in Fig. 4.4.3. There is no appreciable change in peak factor with speed, especially at high power level. Peak factor increases with a reduction in the load power. At lower speeds the variation of peak factor with varying power is still less pronounced.

Power remaining the same, the ripple factor increases with an increase in the speed. It increases with a decrease in power levels over the entire speed range. The increase is more pronounced at higher speeds than at lower speeds.

4.4.3 Supply Harmonic Spectrum

Fig. 4.4.4 shows dominant supply current harmonics. As in the case of the separately excited motor load, the spectrum of supply current harmonics has shifted from lower order to higher order frequency components. Because of the three-phase supply, the triplen harmonics are absent. The dominant harmonics are eleventh and thirteenth. They are quite significant at low speed but decrease gradually as the speed increases. With the exception of eleventh and thirteenth, the variation in other harmonics as the power level changes, is not quite significant over the entire speed range. Owing to the lack of half-

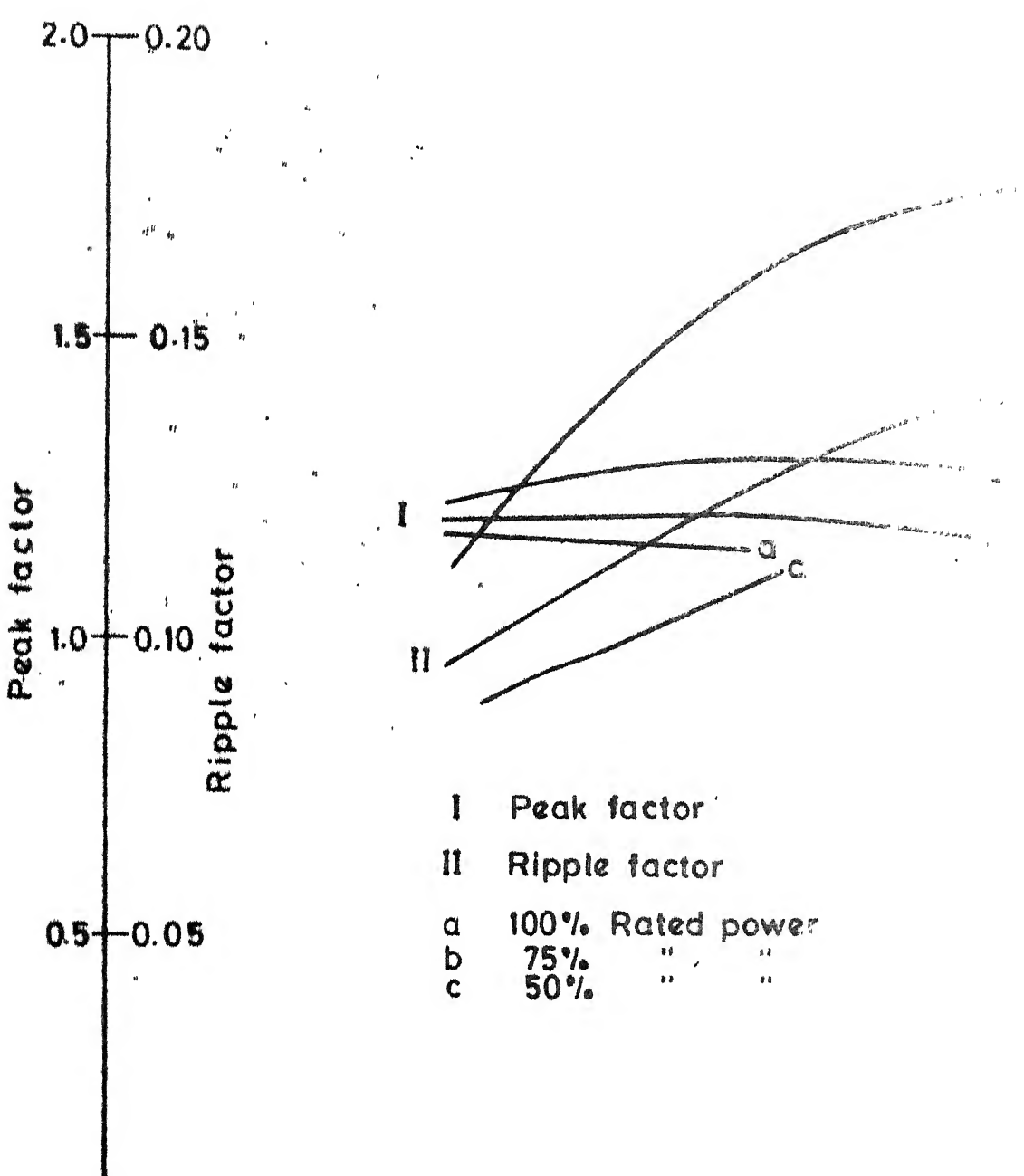

IG. 4.4.3 VARIATION OF PEAK FACTOR AND RIPPLE FACTOR WITH SPEED FOR CONSTANT POWER OPERATION

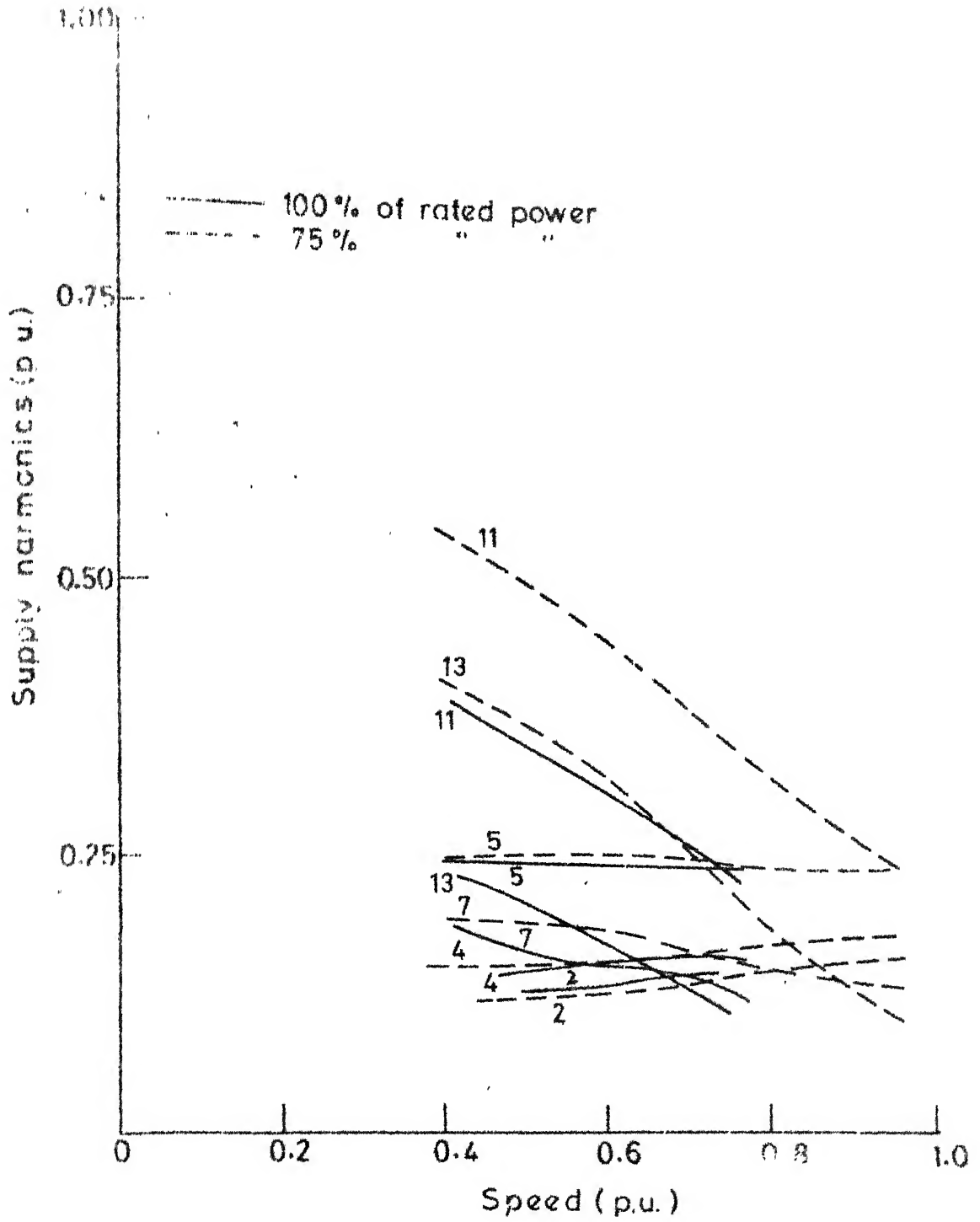

FIG 4.4.4 VARIATION OF SUPPLY HARMONICS IN P.U. OF FUNDAMENTAL CURRENT WITH SPEED FOR CONSTANT POWER OPERATION

wave symmetry in the source current even harmonics are also generated. Among these, the fourth and second harmonics are in smaller proportions compared to dominant odd harmonic currents. The other higher order even harmonics are of still lower magnitudes. These harmonics are not shown in Fig. 4.4.4.

4.5 EXPERIMENTAL OSCILLOGRAMS

Experimental oscillograms are illustrated in Fig. 4.5.1. Commutation transients for different pulses are shown at 0.7 modulation index with the motor running at 900 rpm. These oscillograms illustrate the basic principles of operation of the converter and verify the working of the circuit including commutation interval. From an observation of these waveforms, sequence of mode change can be determined. Commutation transients due to the bottom group thyristors (T_4-T_6) can also be seen in these experimental oscillograms.

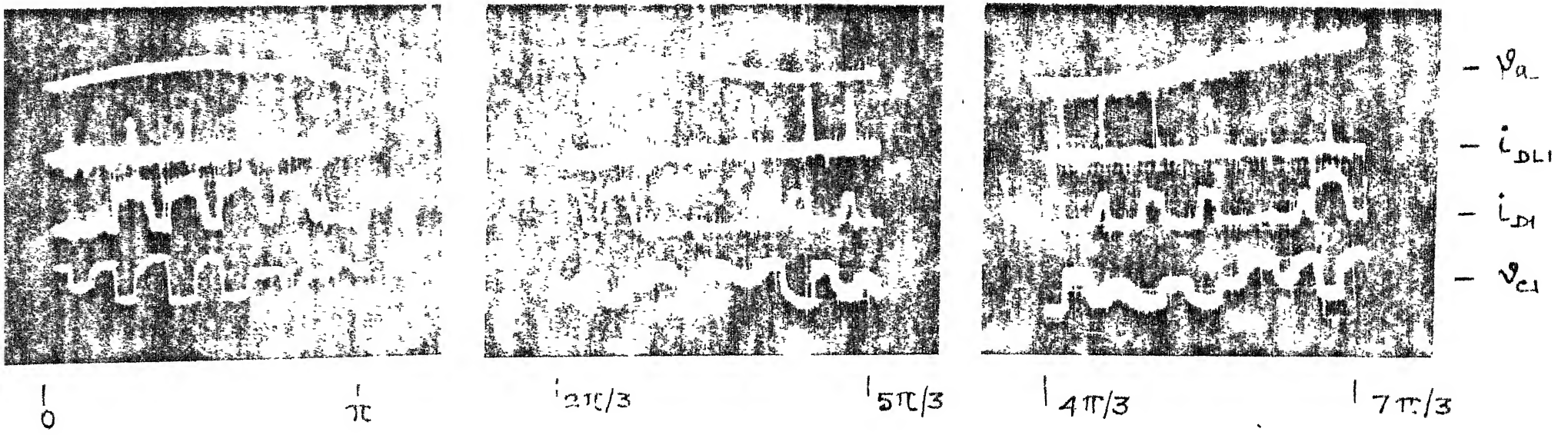

Fig 4.5.1 (a)

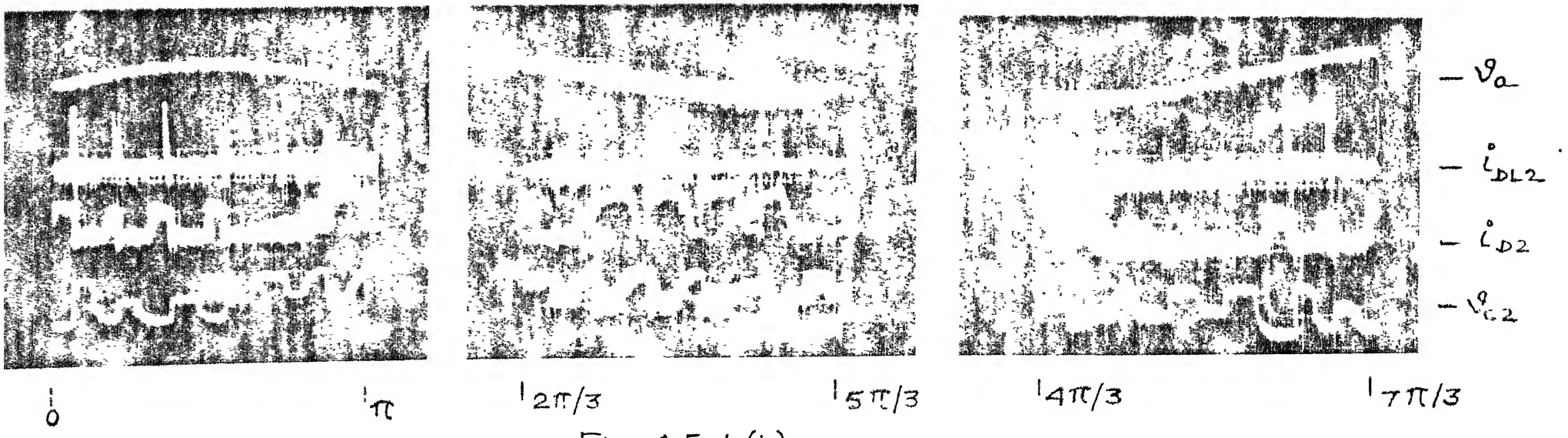

Fig 4.5.1 (b)

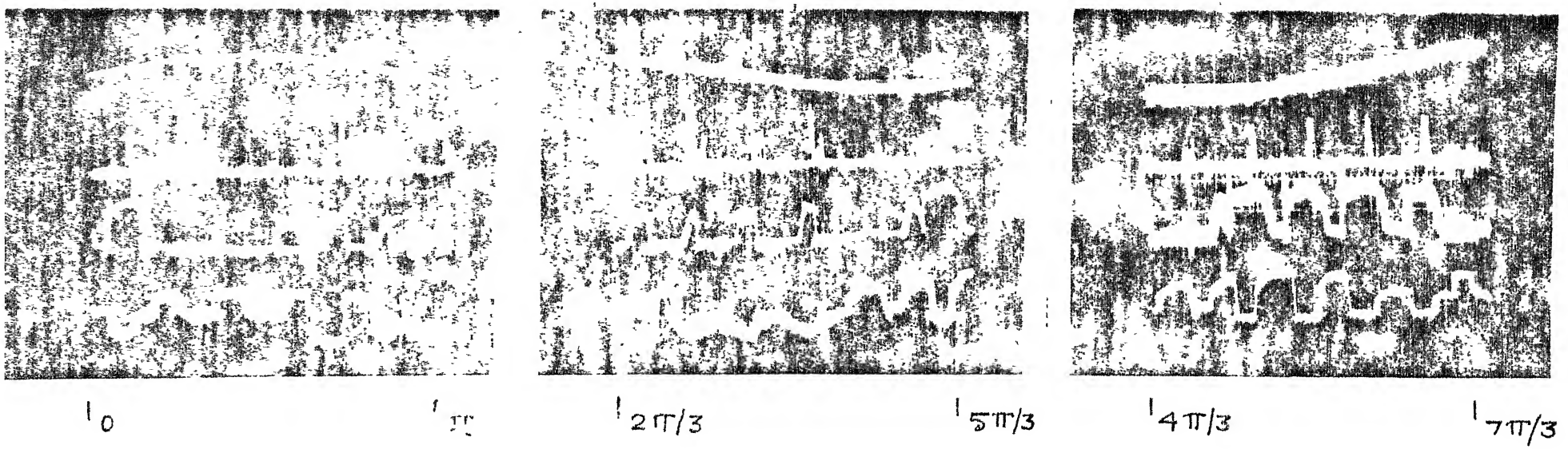

Fig 4·5·1 (c)

Fig 4·5·1 Scale : v_a = 500 V/div

i_{DL} = 29·41 A/div

i_D = 2·44 A/div

v_c = 200 V/div

Time = 1 msec/div.

CHAPTER V

CONCLUSIONS

5.1 CONCLUSIONS

Even with no additional inductance in the armature circuit, the range of continuous conduction in the speed torque plane is much larger in case of a three-phase ac-dc SPWM converter than that in case of a phase-controlled converter. This feature is particularly important for motors of inherently low inductance. The ripple factor and the peak factor are improved. As a result of an improvement in the ripple factor, the armature copper loss decreases and the efficiency of the converter motor drive system is improved. The decrease in the peak factor has a beneficial effect on the machine commutation and thyristor ratings.

The power factor is also improved. The displacement factor is held at unity over the entire range of the output voltage.

Because of sinusoidal multipulse width modulation, there is a shift in the supply harmonic spectrum from lower order to higher order. The higher order harmonics can be easily filtered out by small sized filter components. Though the SPWM scheme has generated even harmonics in the supply system, these harmonics are of low amplitude and remain almost constant over the entire range of speed.

The above discussions are true for both the dc series and separately excited motors.

The digital firing scheme provides accurate and precise firing besides being highly stable. By mere change of the look-up table, PWM technique of any strategy can be implemented.

The converter circuit is quite versatile since rectification and inversion operations can be easily achieved without any modification in the converter circuit configuration. Compared to a line commutated full converter this converter circuit requires some additional investment on three power diodes, three commutating capacitors, three commutating inductors and three commutating diodes. But in comparison with the phase-controlled converter, the improved performance characteristics make the three-phase 3PWM converter attractive for industrial applications involving dc drives of medium and large power ratings.

The experimental results have been verified. Analysis of the converter is somewhat complex because of forced commutation. Additional modes of operation which occur due to the commutation of bottom group thyristors (T_4-T_6) can be observed in the experimental oscillograms.

5.2 SCOPE OF FURTHER WORK

The performance of a three-phase SPWM converter-fed dc series motor running in reverse regeneration can be investigated. For optimum performance of the converter drive system dual mode control strategy using Equal Pulse Width Modulation (EPWM) and SPWM can also be implemented. To eliminate the higher order harmonics, suitable filters can be designed and performance of the system with the filter can be studied. Also a closed loop scheme for the speed control of a dc drive fed from a three-phase ac-dc SPWM converter can be implemented. Four quadrant operation of dc drives using dual-PWM converter can also be a field of research interest.

APPENDIX A

DETERMINATION OF THE MAGNETISATION CHARACTERISTICS OF THE DC SERIES MOTOR

The relationship of the mutual inductance, M_{af} between the armature and field of a dc series motor with the field current, i is assumed to be a fifth degree polynomial equation as is shown in equation (4.2.1). The coefficients C_o to C_5 in equation (4.2.1) are obtained by fitting a fifth degree polynomial curve [18] into the magnetisation characteristics obtained experimentally.

$$C_o+C_1 i+C_2 i^2+C_3 i^3+C_4 i^4+C_5 i^5 = M_{af} \qquad (A1)$$

Each term in the equation (A1) is added to the respective terms in the same equation for n experimental observations. This gives the following equation

$$nC_o+C_1\Sigma_i+C_2\Sigma_i^2+C_3\Sigma_i^3+C_4\Sigma_i^4+C_5\Sigma_i^5 = \Sigma M_{af} \qquad (A2)$$

Multiplying equation (A1) by i and summing them up for n experimental points we get

$$C_o\Sigma_i+C_1\Sigma_i^2+C_2\Sigma_i^3+C_3\Sigma_i^4+C_4\Sigma_i^5+C_5\Sigma_i^6 = \Sigma(M_{af} i) \qquad (A3)$$

Similarly multiplying equation (A1) successively by i^2, i^3 etc. upto i^5 and adding up the terms for all the n points obtained experimentally we get the following set of equations.

$$C_o\Sigma i^2+C_1\Sigma i^3+C_2\Sigma i^4+C_3\Sigma i^5+C_4\Sigma i^6+C_5\Sigma i^7 = \Sigma(M_{af}\ i^2) \quad (A4)$$

$$C_o\Sigma i^3+C_1\Sigma i^4+C_2\Sigma i^5+C_3\Sigma i^6+C_4\Sigma i^7+C_5\Sigma i^8 = \Sigma(M_{af}\ i^3) \quad (A5)$$

$$C_o\Sigma i^4+C_1\Sigma i^5+C_2\Sigma i^6+C_3\Sigma i^7+C_4\Sigma i^8+C_5\Sigma i^9 = \Sigma(M_{af}\ i^4) \quad (A6)$$

$$C_o\Sigma i^5+C_1\Sigma i^6+C_2\Sigma i^7+C_3\Sigma i^8+C_4\Sigma i^9+C_5\Sigma i^{10} = \Sigma(M_{af}\ i^5) \quad (A7)$$

Equations (A2) to (A7) give a set of simultaneous linear equations of coefficients C_o to C_5

$$\begin{bmatrix} n & \Sigma i & \Sigma i^2 & \Sigma i^3 & \Sigma i^4 & \Sigma i^5 \\ \Sigma i & \Sigma i^2 & \Sigma i^3 & \Sigma i^4 & \Sigma i^5 & \Sigma i^6 \\ \Sigma i^2 & \Sigma i^3 & \Sigma i^4 & \Sigma i^5 & \Sigma i^6 & \Sigma i^7 \\ \Sigma i^3 & \Sigma i^4 & \Sigma i^5 & \Sigma i^6 & \Sigma i^7 & \Sigma i^8 \\ \Sigma i^4 & \Sigma i^5 & \Sigma i^6 & \Sigma i^7 & \Sigma i^8 & \Sigma i^9 \\ \Sigma i^5 & \Sigma i^6 & \Sigma i^7 & \Sigma i^8 & \Sigma i^9 & \Sigma i^{10} \end{bmatrix} \begin{bmatrix} C_o \\ C_1 \\ C_2 \\ C_3 \\ C_4 \\ C_5 \end{bmatrix} = \begin{bmatrix} \Sigma(M_{af}) \\ \Sigma(M_{af} i) \\ \Sigma(M_{af} i^2) \\ \Sigma(M_{af} i^3) \\ \Sigma(M_{af} i^4) \\ \Sigma(M_{af} i^5) \end{bmatrix} \quad (A8)$$

Several values of M_{af} are obtained arexperimentally by noting down the armature voltage induced at a known speed with different values of field currents, the motor being run as a separately excited dc generator. With 'n' such values of M_{af} and i the set of equations (A8) is solved to give the coefficients C_o to C_5 of equation (4.2.1).

APPENDIX B

DETAILS OF THE EXPERIMENTAL SET UP

Converter Components

Thyristors T_1, T_2, T_3	: Inverter grade (Turn-off time = 12 μsec.) Type : T12FCDC 1000
Thyristors T_4, T_5, T_6	: Converter grade Type : 36TB12
Diodes D_1, D_2, D_3	: S15 HR 25
Diodes D_{L1}, D_{L2}, D_{L3}	: S 15 HR 70
Inductors L_{C1}, L_{C2}, L_{C3}	: 0.1 m Herys
Inductors L_s	: 0.4 m Herys
Capacitors C_1, C_2, C_3	: 8 μFd.

Parameters of Separately Excited DC Motor

Rated Power	: 3 HP
Rated Voltage	: 220 Volts
Rated Current	: 11.6 Amps.
Rated Speed	: 1450 RPM
Armature Resistance	: 2.25 Ohms
Armature Inductance	: 0.0228 Henrys
Back EMF Constant	: 1.378 Volts/(rad)

Parameters of DC Series Motor

Rated Power	: 3 HP
Rated Voltage	: 220 Volts
Rated Current	: 11.6 Amps.
Rated Speed	: 1500 RPM
Total Resistance	: 2.6 Ohms
Total Inductance	: 25 nHenrys

REFERENCES

[1] A. McMurray, 'A study of asymmetrical gating for phase-controlled converters', IEEE Trans. Ind. Appl., vol. IA-8, p 289, 1972.

[2] S. Mukhopadhyay, 'A new concept for improving the performance of phase-controlled converters', IEEE Trans. Ind. Appl., vol.IA-14, p 584, 1978.

[3] V.R. Stefanovic, 'Power factor improvement with a modified phase-controlled converter', IEEE Trans. Ind. Appl., vol.IA-15, p. 193, 1979.

[4] T. Ohnishi and H. Okitsu, 'Bias voltage controlled three-phase converter with high power factor', IEEE Trans. Ind. Appl., vol. IA-16, p.700, 1980.

[5] C. Nagamani, 'A three-phase ac to dc SPWM converter controlled dc motor drive', M.Tech. thesis, Deptt. of Elect. Engg., IIT Kanpur, Dec. 1983.

[6] K.A. Krishnamurthy, G.K. Dubey and G.N. Revankar, 'Analysis of ac chopper-fed dc series motor', Institute of Engineers (I) Journal-EL, vol.59, 1, Aug. 1978.

[7] P. Mehta, S. Mukhopadhyay and E. Orhun, 'Forced commutated ac-dc converter-controlled dc drives', IEEE Conf. on Power Electronics-Power Semiconductors and Their Applications, Conf. Pub. 123, p 146, 1974.

[8] K.A. Krishnamurthy, G.N. Revankar and G.K. Dubey, 'General Method for Selective reduction of line harmonics', Proc. IEE, p 321, Nov. 1978.

[9] P.C. Sen and S.R. Doradla, 'Symmetrical and extinction angle control of solid state series motor drive', IEEE Trans. IECI, vol. 23, p 31, 1976.

[10] T. Kataoka, K. Mizumachi and S. Miyairi, 'A pulse-width controlled ac to dc converter to improve power factor and waveform of ac line current', IEEE Trans. Ind. Appl., vol. IA-15, p 670, 1979.

[11] H.K. Patel and G.K. Dubey, 'Firing scheme for pulse width controlled ac-dc converters', Int. J. Electronics, vol.52, No.5, p 447, 1982.

[12] P.D. Parikh and S.R. Doradla, 'Equal pulse-width modulation control strategy for an ac to dc converter', Int. J. Electronics, vol. 55, No.3, p 339, 1983.

[13] N.V.P.R. Durga Prasad, S.R. Doradla and Y.V.V.S. Murthy, 'Versatile digital firing schemes for pulse-width modulated ac-dc converters', Conf. Records, Annual Meeting of IEEE Ind. Appl. Soc., 826, 1984.

[14] P.C. Sen, 'Thyristor DC Drives', New York: John Wiley and Sons, 1982.

[15] P.D. Damle and G.K. Dubey, 'Analysis of chopper-fed dc series motor', IEEE Trans., vol. IECI-23, No.1, p 92, 1976.

[16] P.W. Franklin, 'Theory of the dc motor controlled by power pulses', IEEE Trans., vol. PAS-91, p 249, 1972.

[17] G.K. Dubey and W. Shepherd, 'Analysis of series motor controlled by power pulses', Proc. IEE, vol.122, No. 12, p 1397, 1975.

[18] Henry Margenau and G.M. Murphy, 'The Mathematics of Physics and Chemistry', 2nd Edn., Affiliated E.W. Press Pvt.Ltd., New Delhi.

[19] S.R. Doradla, C. Nagamani and Subhankar Sanyal, 'A sinusoidal pulse width modulated three-phase ac to dc converter-fed dc motor drive', Conf. Records, Annual Meeting of IEEE Ind. Appl. Soc., p 668, 1984.